INTERNATIONAL ATOMIC ENERGY AGENCY

INDC(NDS)-0470
Distr. AC

I N D C INTERNATIONAL NUCLEAR DATA COMMITTEE

Thermal Neutron Scattering Data for the Moderator Materials H_2O, D_2O and ZrH_x in ENDF-6 Format and as ACE Library for MCNP(X) Codes

Prepared by

M. Mattes and J. Keinert

Institute for Nuclear Technology and Energy Systems (IKE) – University of Stuttgart
Pfaffenwaldring 31, P.O.Box 801140, D-70550 Stuttgart, Germany

April 2005

IAEA NUCLEAR DATA SECTION, WAGRAMER STRASSE 5, A-1400 VIENNA

INDC documents may be downloaded in electronic form from
http://www-nds.iaea.or.at/indc_sel.html or sent as an e-mail attachment. Requests for hardcopy or e-mail transmittal should be directed to services@iaeand.iaea.org or to:

Nuclear Data Section
International Atomic Energy Agency
PO Box 100
Wagramer Strasse 5
A-1400 Vienna
Austria

Produced by the IAEA in Austria
April 2005

INDC(NDS)-0470
Distr. AC

Thermal Neutron Scattering Data for the Moderator Materials H_2O, D_2O and ZrH_x in ENDF-6 Format and as ACE Library for MCNP(X) Codes

Prepared by

M. Mattes and J. Keinert

Institute for Nuclear Technology and Energy Systems (IKE) – University of Stuttgart
Pfaffenwaldring 31, P.O.Box 801140, D-70550 Stuttgart, Germany

ABSTRACT

At thermal neutron energies, the binding of the scattering nucleus in a solid, liquid, or gas affects the cross section and the angular and energy distributions of the scattered neutrons. These effects are described in the thermal sub-library of evaluated files in File 7 of the ENDF-6 format.

New and re-evaluations are described for the three thermal moderator materials: hydrogen bound in light water (H_2O), deuterium bound in heavy water (D_2O) and hydrogen in ZrH (zirconium hydride). The calculations for a variety of temperatures were made with the LEAPR module of NJOY to obtain new evaluated thermal neutron scattering files that are accurate over a wider range of energy and momentum transfer than existing files. The IKE physics models are described in detail, and the inputs to LEAPR are given.

Detailed comparisons with a significant number of measurements of differential and integral neutron cross sections and other relevant data are reported (for the validation of the generated Scattering Law data files $S(\alpha,\beta,T)$). Experimental data are reproduced reasonably well. In addition, thermal MCNP data sets for use in the continuous Monte Carlo codes MCNP and MCNPX were generated from these evaluations. Calculated neutron spectra agree rather well with measurements.

Details are also given of the updates to the NJOY modules LEAPR, THERMR, and ACER necessary in generating and processing the thermal neutron scattering data.

April 2005

Table of Contents

List of Figures

List of Tables

1 Introduction

At thermal neutron energies, the binding of the scattering nucleus in a solid, liquid or gas moderator material affects the neutron cross section and the energy and angular distribution of secondary neutrons, as the neutron can give up energy to excitations in the material, or can gain energy. In the evaluated nuclear data files (ENDF/B-VI and JEF-2.2), these effects are described in the thermal sub-library using the File 7 format [1].

Status of Thermal Neutron Scattering Data

- The majority of the work on thermal neutron scattering was performed in the 1950s and 1960s
- Subsequently (1970s), data libraries were generated mainly using the GASKET methodology, which was developed at General Atomic (GA) [2, 3]
- New ENDF files that are accurate over a wider range of energy and momentum transfer than the existing files were calculated with the scattering law module LEAPR [4] (implemented in the early 1990s in the nuclear data processing system NJOY [5]) which uses methods based on the British code LEAP, together with the original GA physics models
- To date, this is the only set of data that is available as part of the ENDF/B-VI libraries
- In JEF-2.2 the Scattering Law data are carried over from JEF-1 (1984) [6]. The models for the neutron scattering of H in light water H_2O and D in heavy water D_2O were developed at IKE and the generation of $S(\alpha,\beta)$ was done using GASKET-2.
- The LANL report on LEAPR [4] shows that there is reasonable agreement between LEAPR and GASKET results. This is also the experience at IKE after modifications of the code GASKET-2.
- Work started at IKE in 2003 to re-evaluate and review the currently used thermal scattering law data $S(\alpha,\beta)$ for H_2O, D_2O and ZrH_x as a function of temperatures equal to or greater than room temperature. This includes updating of models and model parameters, using LEAPR for the generation of $S(\alpha,\beta)$ with more details in the α and β grids and higher energy transfer, the processing of the generated $S(\alpha,\beta)$ with NJOY and the comparison with measurements for differential and integral thermal neutron cross sections as well as neutron spectra.
- Documentation of the results was completed in 2004.

Newer experimental data for the verification of generated thermal neutron scattering data are very scarce. Measurements were mainly done in the 1960s, especially at GA and RPI in USA, in UK and in Germany in the research centres of Jülich and Karlsruhe.

2 Thermal Neutron Scattering

The thermal neutron scattering cross section is usually divided into three different parts:

- **Inelastic**: Important for all materials (both incoherent and coherent inelastic fall in this category) and described by the scattering law S(α,β).
- **Incoherent elastic**: Important for hydrogenous solids like zirconium hydride and polyethylene or light water ice.
- **Coherent elastic**: Important for crystalline solids like graphite, beryllium or UO_2.

2.1 Inelastic Scattering

In standard references or in the LEAPR documentation in [4] it is shown that the double differential scattering cross section for thermal neutrons for gases, liquids, or solids consisting of randomly ordered atoms or molecules (principle scatterer) can be written as

$$\frac{d^2\sigma}{d\Omega dE'}(E \to E', \Omega \to \Omega') = \frac{\sigma_b}{4\pi\, kT}\sqrt{\frac{E'}{E}}\, e^{-\frac{\beta}{2}}\, S(\alpha,\beta)$$

where E and E' are the incident and secondary neutron energies in the laboratory system, Ω is the scattering angle in the laboratory system, σ_b is the bound scattering cross section for the material (sum of $\sigma_b^{inc} + \sigma_b^{coh}$), kT is the temperature in eV, and S(α,β) is the symmetric form of the thermal scattering law. The scattering law depends on only two variables:

- the momentum transfer κ

$$\alpha = \frac{E'+E-2\sqrt{E'E}\cos\theta}{A\,kT} = \frac{\hbar^2\kappa^2}{2M\,kT}$$

  where A is the ratio of the mass of the scattering atom M to the neutron mass, and

- the energy transfer ε

$$\beta = \frac{E'-E}{kT} = \frac{\varepsilon}{kT}$$

The asymmetric scattering law is the Fourier transform of the intermediate scattering function

$$e^{-\frac{\beta}{2}} S(\alpha,\beta) = \frac{1}{2\pi\hbar}\int_{-\infty}^{\infty} e^{\frac{i\varepsilon t}{\hbar}}\, \chi(\kappa,t)\, dt$$

For a medium with isotropic neutron scattering this scattering function is given in the Gaussian approximation by

$$\chi(\kappa,t) = \exp\left[\frac{\hbar^2\kappa^2}{2M}\left(-\int_0^{\infty}\frac{\rho(\omega)}{\hbar\omega}\coth\frac{\hbar\omega}{2kT}\,d\omega + \int_0^{\infty}\frac{\rho(\omega)}{\hbar\omega}\left(\coth\frac{\hbar\omega}{2kT}\cos\omega t + i\sin\omega t\right)d\omega\right)\right],$$

with $\rho(\omega)$ as the generalised frequency spectrum of excitations in the system expressed as a function of ω, where the spectrum must be normalised as follows

$$\int \rho(\omega)d\omega = 1$$

The frequency spectrum is decomposed into a sum of simple excitation spectra

$$\rho(\omega) = \sum_{i=1}^{K} \rho_i(\omega)$$

where the following possibilities are allowed in the codes LEAPR and GASKET:

$\rho_i(\omega) = \rho_t(\omega) = w_t\,\delta(\omega)$	translational spectrum
$\rho_i(\omega) = \rho_d(\omega)$	diffusion
$\rho_i(\omega) = \rho_s(\omega)$	solid-type spectrum (broad band of ω)
$\rho_i(\omega) = w_j\,\delta(\omega-\omega_j)$	discrete oscillator at ω_j

The solid-type spectrum must vary as ω^2 as ω goes to zero, and it must integrate to w_s the weight for the solid-type law. The translational spectrum must integrate to w_t, the translational weight.
In this formalism the inelastic scattering of thermal neutrons is treated in incoherent approximation as the bound scattering cross section is taken as the sum of $\sigma_b^{inc} + \sigma_b^{coh}$. To take into consideration the coherent inelastic neutron scattering in liquids see section 2.5.

2.2 Short-Collision-Time Approximation

For high incident energies, α and/or β values may be required that are outside the ranges of tabulated $S(\alpha,\beta)$. In these cases, the short-collision-time (SCT) approximation should be used for the deep inelastic scattering of thermal neutrons as follows:

$$S^{SCT}(\alpha,\beta,T) = \frac{e^{-\left[\frac{(\alpha-|\beta|)^2 T}{4\alpha T_{eff}(T)} + \frac{|\beta|}{2}\right]}}{\sqrt{4\pi\alpha \frac{T_{eff}(T)}{T}}}$$

where the effective temperature $T_{eff}(T)$ is correlated to the generalised frequency distribution $\rho(\omega)$ according to

$$T_{eff} = \frac{1}{2}\int_0^{\omega_{max}} \hbar\omega \coth\frac{\hbar\omega}{2kT}\rho(\omega)\,d\omega$$

It is important to mention that the principle of detailed balance is forced in the formula for the short-collision-time approximation (SCTA).

2.3 Incoherent Elastic Scattering

In hydrogenous solids there is an elastic (no energy change) component of scattering. In ENDF terminology this is called the "incoherent elastic" term.

The corresponding differential scattering cross section is

$$\frac{d^2\sigma}{d\Omega dE'} = \frac{\sigma_b}{4\pi}\exp(-2E(1-\mu)\frac{\gamma(0)}{A})\delta(\mu)\delta(E-E')$$

and the integrated scattering cross section is

$$\sigma(E) = \frac{\sigma_b A}{4E\,\gamma(0)}[1-\exp(-4E\frac{\gamma(0)}{A})]$$

where the Debye-Waller integral $\gamma(0)$ is computed from the frequency spectrum as

$$\gamma(0) = \int_0^{\omega_{\max}} \frac{\rho(\omega)}{\hbar\omega}\coth\frac{\hbar\omega}{2\,kT}\,d\omega$$

The bound scattering cross section σ_b and the Debye-Waller integral divided by the reduced atomic mass ($=\gamma(0)/A$) are given as a function of temperature in the section MF=7 and MT=2 in the ENDF-6 format.

2.4 Coherent Elastic Scattering

In solids consisting of coherent scatterers, interference scattering from the various planes of atoms of the crystals making up the solid occurs. The ENDF term for this process is "coherent elastic scattering" as there is no energy loss.
The differential coherent elastic scattering cross section for polycrystalline materials is given by

$$\frac{d^2\sigma_{coh}}{d\Omega dE'}(E\to E',\Omega\to\Omega') = \frac{\sigma_b}{E}\sum_{E_i<E} f_i\, e^{-4\gamma(0)E_i/A}\delta(\mu-\mu_i)\delta(E-E')$$

where

$$\mu_i = 1-\frac{2E_i}{E}$$

and the integrated cross section is given by

$$\sigma_{coh} = \frac{\sigma_b}{E}\sum_{E_i<E} f_i e^{-4\gamma(0)E_i/A}$$

σ_b is the effective bound coherent scattering cross section for the material, E_i are the so-called "Bragg edges", and the f_i are related to the crystallographic structure factors.

The coherent elastic cross section is zero below the first Bragg edge E_1 (typically 2 to 5 meV). The quantity $E_i\sigma_{coh}(E_i)$ as a function of energy and temperature is stored in the ENDF-6 format in MF=7 and MT=2. The knowledge of the crystal structure of the scattering material

is necessary to calculate the E_i and f_i. The methods used in LEAPR are taken over from HEXSCAT. Crystal structures other than hexagonal are added to LEAPR:

2.5 Intermolecular Neutron Interference Scattering in Liquids

In general the thermal neutron scattering can be formulated as

$$S(\alpha,\beta) = \frac{\sigma^{inc}}{\sigma} S^{inc}(\alpha,\beta) + \frac{\sigma^{coh}}{\sigma} S^{coh}(\alpha,\beta)$$

with $\sigma = \sigma^{inc} + \sigma^{coh}$

According to the formalism by Van Hove [7] the incoherent scattering is a part of the self term S_s and the distinct coherent part S_d is caused by intermolecular interference scattering. In calculating S^{coh} for liquids various approximations are in use:

- **Incoherent approximation** ($S_d \equiv 0$) $S^{coh}(\alpha,\beta) = S^{inc}(\alpha,\beta)$
- **Vineyard approximation [8]** $S^{coh}(\alpha,\beta) = S^{inc}(\alpha,\beta) * S(\kappa)$

  with the static structure factor $S(\kappa)$
- **Sköld approximation [9]** $S^{coh}(\alpha,\beta) = S^{inc}(\alpha',\beta) * S(\kappa)$

  with $\alpha' = \alpha/S(\kappa)$

Among these approximations the back-scattering of the interacting molecule is best described by the Sköld approximation.

2.6 Free Gas

For a free gas of scatterers with no internal structure the frequency distribution degenerates into $\rho(\omega) = 1/A * \delta(0)$ and the scattering law is then given by

$$S(\alpha,\beta) = \frac{e^{-\frac{\alpha^2+\beta^2}{4\alpha}}}{\sqrt{4\pi\alpha}} .$$

3 Generation of S(α,β) - Processing of Thermal Neutron Scattering Data

The LEAPR module of NJOY is used to prepare the scattering law S(α,β) and related quantities, which describe thermal neutron scattering from bound moderators, in the ENDF-6 format used by the THERMR module of NJOY.

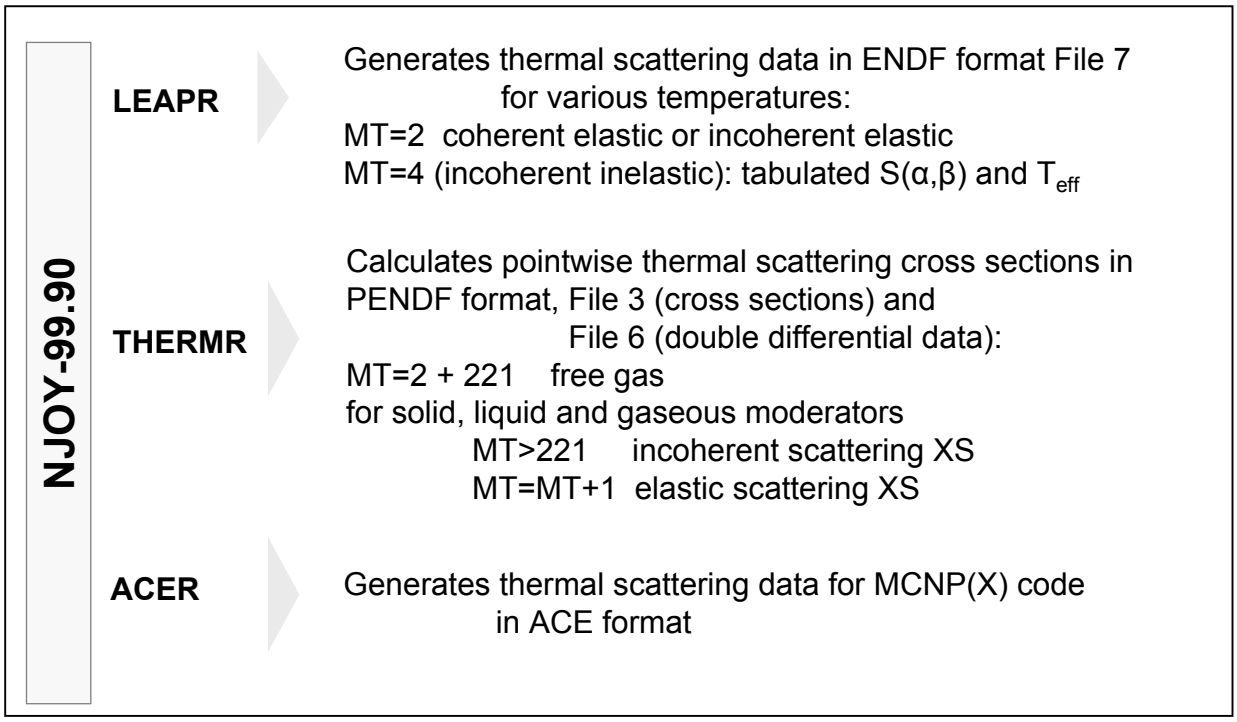

Figure 3.1 NJOY modules for the generation of thermal neutron scattering data for application

For binding in solids and liquids, the scattering law S(α,β) is given in ENDF format File 7 as tables of S versus α for various values of β. Values of S for other values of α and β can be obtained by interpolation. The scattering law is normally symmetric in β and only has to be tabulated for positive values, but for materials like ortho-hydrogen and para-hydrogen of interest for cold moderators, this is not true as the principle of detailed balance is not fulfilled.

If the α or β required is outside the range of the table in File 7, the differential scattering cross section is computed in THERMR using the short-collision-time approximation (SCTA). The effective temperatures T_{eff} needed are included in the data file.

THERMR expects the requested temperature T to be one of the temperatures included on the ENDF thermal file, or within a few degrees of that value. Intermediate temperatures should be obtained

- by interpolating between the resulting cross sections and not by interpolating S(α,β) or
- by running LEAPR for the wanted temperature T.

3.1 General Remarks on the Choice of the α, β -grid for the Scattering Law Tables

The choice of the α,β-grid has to be oriented towards the peak structure of the generalised frequency distribution ρ(ω) of the scattering nucleus to assure resonance scattering of the thermal neutrons in the system of bound moderator atoms. The α,β-grid must consider multi-phonon excitations of the individual peaks, the minima in ρ(ω) as well as combinations of the peaks of different modes because these are independent motions (known as sum of excitation levels).
In the past (JEF-1 or ENDF/B-III) the strong correlation of neutron energy transfer with excitation of the dynamical modes of individual scattering nucleus was not always considered.

The maximum values of the α,β-grid were often treated somehow arbitrarily. In the theoretical formulation for the calculation of thermal neutron scattering cross sections the frequency distribution ρ(ω) is treated in the harmonic approximation. This implies that a parabolic potential is taken for the harmonic oscillators allowing excitations up to infinity. The realistic potential is unharmonic. Therefore possible excitations are limited by the binding energy E_b of the scattering nucleus in the molecule or lattice structure. Therefore the maximum values in the α,β-grid should be taken as

$$\beta_{max} = E_b / kT$$

$$\alpha_{max} = 4\,\beta_{max} / A$$

in a consistent set and the maximum energy transfer E_{max} is set equal to E_b in the Scattering Law data tables. For greater energy transfers up to the thermal cut-off energy (≤ 5 eV) the neutron interaction is treated within the short collision time approximation (SCTA) as with a free gas of the scattering nuclei with the effective temperature T_{eff} . This extension of the S(α,β) tables is done in the THERMR module in NJOY in the calculation of the double differential neutron scattering cross sections.

Considering this procedure with E_b compared to the older arbitrary treatment, one has the advantage of producing much smaller S(α,β) tables without any loss of accuracy. In addition we do not have to provide the α,β-grid dense enough for large values of α and β to avoid interpolation errors as is demonstrated for dσ/dE for H bound in H_2O in section 4.2 in Figure 4.5.

4 Light Water, H in H_2O

4.1 Model Description

At low energies ($E \leq 4$ eV) the interaction of the scattered neutron with the scattering nucleus is pronounced by the individual dynamical excitations of the scattering nucleus.

The IKE model for water assumes that the scattering law for the primary scatterer (H) is well represented by a set of hindered rotations given as a solid-type frequency distribution (temperature dependent), two discrete oscillators (.205 and .436 eV) to represent the molecular vibrations, and a hindered translational mode with effective temperature dependent masses.

Based on work by Eucken [10] and experimental data by Haywood and Page [12], the modes of the scattering dynamics of H bound in H_2O in the liquid phase are treated as

- hindered translations with effective temperature dependent masses. These values are listed for a grid of temperatures in Table 4.1 and are derived from the work of Eucken [10]. The moving translational units can be thought to be clusters of single molecules as well as of two, four, and eight complexes of H_2O molecules with varying fractions depending on temperature as given in Figure 4.1. This assumption was corroborated later by Bertagnolli [11].
- hindered rotations with a broad band of frequencies, which are temperature-dependent. For a specific temperature, interpolation for the continuous part $\rho(\omega)$ is done between the two limiting curves at 294 and 624 K given in Figure 4.2, based on measurements by Haywood and Page [12]. Also shown in this figure is the temperature independent frequency distribution used in the ENDF model.
- two Einstein δ-oscillators describing the bending and stretching vibrations within the water molecule (see Figure 4.3). Compared to our model for the JEF data the frequency of the degenerated stretching vibrations are slightly reduced from .48 meV to .436 meV taking into account the liquid state (Springer [13]). The numerous values for the frequencies of the intra-molecular oscillations for the three phases (solid, liquid, vapour) are listed in Table 4.2.

For the optical modes it is assumed that each of the six degrees of freedom are equally weighted contrary to the ENDF model [2] [4] and the previous model for JEF [6].

The scattering on oxygen is represented using a free-gas law for mass 16.

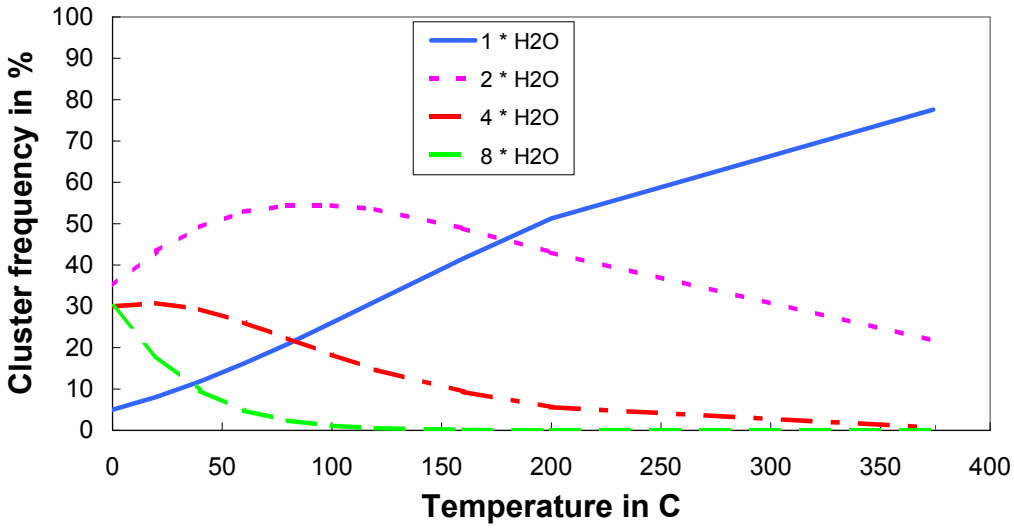

Figure 4.1 Molecular cluster structure of liquid water as a function of temperature (derived from Eucken [10])

Table 4.1 Effective masses M_{trans} for the translational mode, effective temperature T_{eff}, Debye-Waller integral $\gamma(0)$ and the average scattering amplitude $\langle u \rangle$ of H bound in H_2O as a function of temperature T

T in K	**T_{eff}** in K		**$\gamma(0)$** in eV^{-1}		**<u>** in Å		**M_{trans}** in amu	
	IKE	**GA**	**IKE**	**GA**	**IKE**	**GA**	**IKE**	**GA**
293.6	1297.1	1398.5	11.66	10.19	0.269	.252	46.00	18
323.6	1300.7	1406.3	12.16	10.66	0.275	.258	39.00	18
373.6	1308.9	1420.9	13.01	11.48	0.284	.267	31.00	18
423.6	1321.2	1437.4	13.91	12.34	0.294	.277	27.00	18
473.6	1337.2	1455.4	14.85	13.24	0.304	.287	25.00	18
523.6	1354.6	1475.4	15.79	14.16	0.313	.297	23.00	18
573.6	1374.9	1496.6	16.76	15.11	0.323	.307	22.00	18
623.6	1396.5	1519.1	17.73	16.07	0.332	.316	21.00	18
647.2	1407.0	1530.1	18.22	16.53	0.337	.321	20.40	18
800 *	1488.4	1607.1	21.63	19.57	0.367	.349	20.40	18
1000 *	1608.5	1720.9	26.31	23.68	0.404	.384	20.40	18

In Table 4.1 the effective scattering temperature, the Debye-Waller integral and the average scattering amplitude $\langle u \rangle$ of the bound H are given. $\langle u^2 \rangle$ is proportional to the Debye Waller integral $\gamma(0)$. All these parameters are simply correlated to the chosen $\rho(\omega)$.

* This data set is generated with the frequency distribution at the critical temperature of 647,2 K.

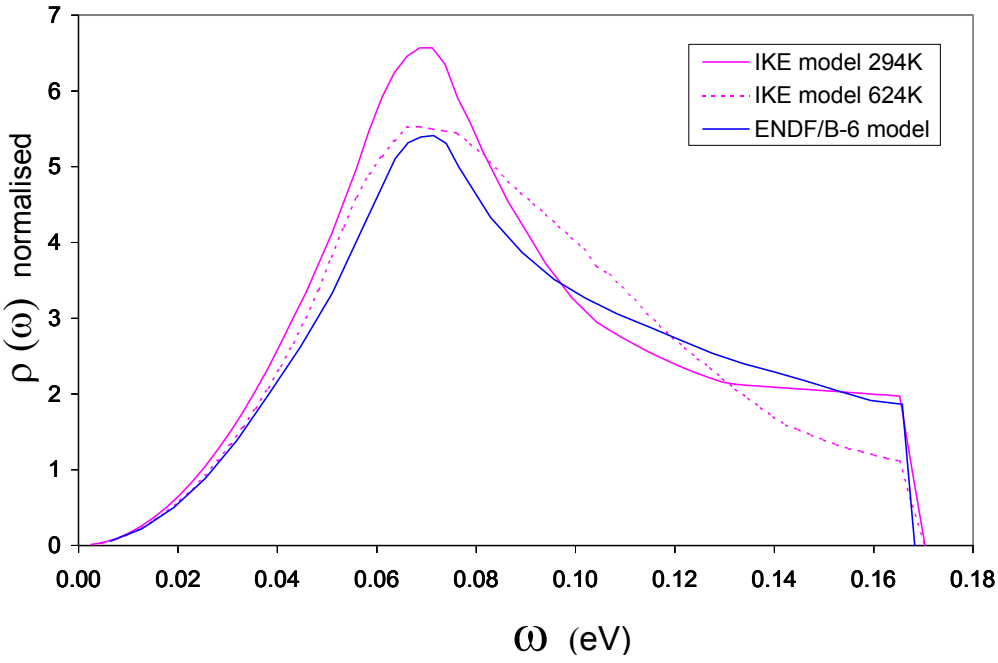

Figure 4.2 Continuous frequency spectra $\rho_s(\omega)$ for two temperatures used for H in H_2O, based on experimental work of Haywood and Page.

Table 4.2 Frequencies ω_j in meV of intra-molecular oscillations of H in H_2O

Oscillations	Ice	Liquid	Vapour
stretching $\omega_{1,3}$	409	436	460
bending ω_2	203	205	198

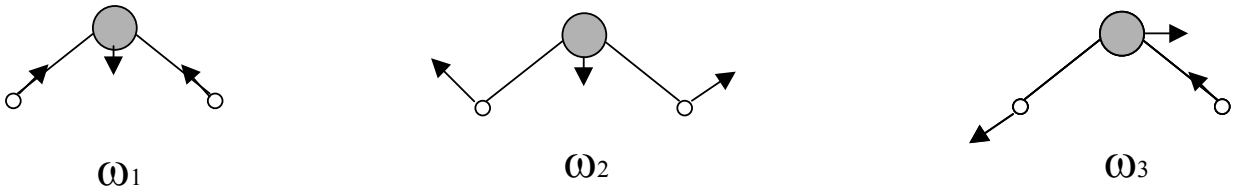

symmetric stretching bending asymmetric stretching

Figure 4.3 Vibrations within a single water molecule H_2O

4.2 LEAPR - Input and Results

The LEAPR module is used to prepare the scattering law S(α,β) and related quantities, which describe thermal scattering from bound moderators, in the ENDF-6 format used by the THERMR module of NJOY.

LEAPR requires a uniform grid for the continuous frequency distribution ρ(ω) for every temperature. The final frequency spectra for the range of temperatures from 293.6 K up to 647.2 K (critical temperature, triple point in the phase diagram) are given in the listed input for LEAPR in the Appendix.

The specific points in the α and β grid were carefully chosen for all dynamical modes and resulted in 182 values for α and 259 values for β. The β grid reflects all the structure in the frequency distribution. As translational modes are to be included, a fine β grid for small β is required to get good results at small α. For the discrete oscillators additional β values are needed at the $n*\omega_i$ (multi-phonon excitations) and their various sums.

The range of β are from zero up to β_{max}=158.1 (equal maximum energy transfer of 4 eV) and that of α from .0005 up to 632.9. In LEAPR the grids are currently limited to 200 elements each, so all arrays for the beta and alpha values have to be increased.

With this choice for the α and β grid, details of the scattering dynamics are well represented in the differential neutron scattering cross section as is given in Figure 4.4.

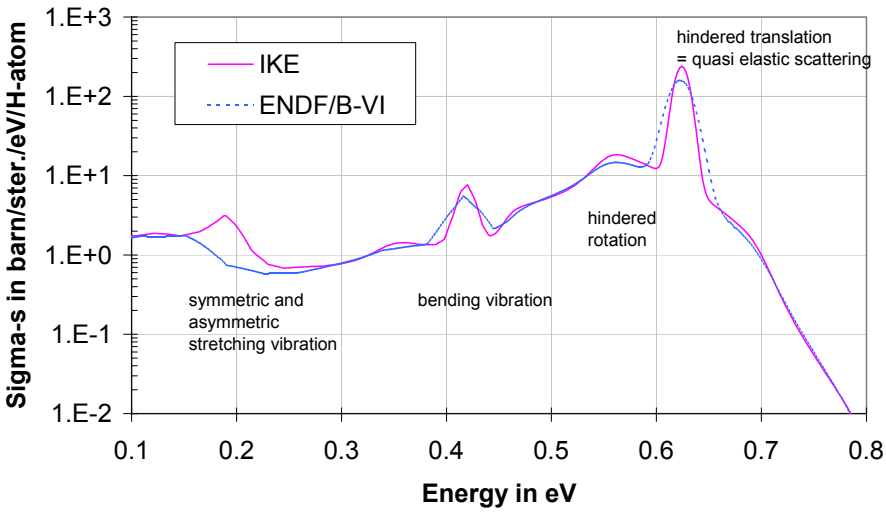

Figure 4.4 Spectra of secondary energies for double differential neutron scattering cross section of H in H_2O (E_i=625 meV at an angle of 15 degree)

In Figure 4.4 the peak structure around the initial neutron energy describes the quasi-elastic domain where hindered or free translations of the hydrogen can be excited. The peak around 560 meV corresponds to the interaction with the hindered rotations of the hydrogen, whereas the peaks around 420 meV and 190 meV are clearly correlated to the bending and stretching vibrations of the bound hydrogen.

The domain of the stretching vibrations are not so pronounced for ENDF/B-VI data. The reason may be in the α and β grid and a higher frequency for these vibrations.

A reduction of about 50 % in the number of the α and β values can be achieved without any loss of accuracy by using a lower value for E_{max} as given in the following table and shown in Figure 4.5. The energy E_b of 1.48 eV corresponds to the binding energy of the single proton in a water molecule [14] [15].

Table 4.3 Maximum energy transfer E_{max} and the numbers of α and β values used in different evaluated files for S(α,β) of H in H2O

Data	E_{max} eV	Number of α values	Number of β values
IKE-IAEA	4	259	182
ENDF/B-VI	4.048	95	97
IKE with $E_{max}=E_b$	1.48	178	137

The interrelation between E_{max} and the short collision time approximation SCTA as calculated by THERMR is demonstrated in Figure 4.5 as an example for the differential neutron scattering probability for H bound in H_2O at an incident neutron energy of 4.46 eV at room temperature (RT).

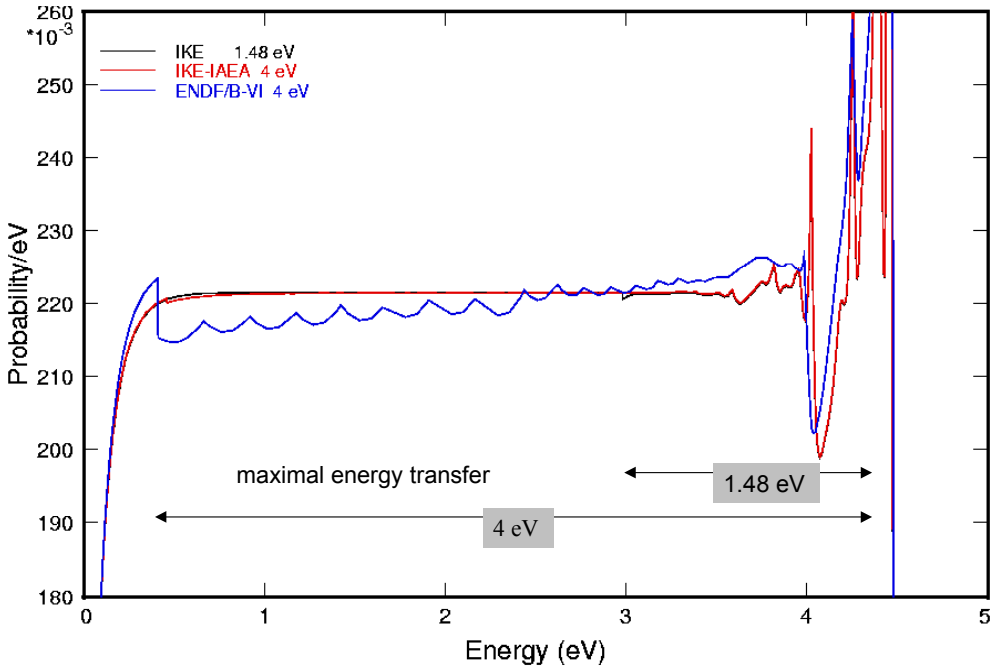

Figure 4.5 Differential neutron scattering probability of H in light water from different evaluated S(α,β) files (E_i = 4.46 eV, RT)

For an incident energy of 4.46 eV the neutron scattering cross section is 20.77 barn for both IKE evaluations whereas the ENDF/B-VI file yields a value of 20.36 barn which seems to be too low. The free atomic neutron scattering cross section is 20.478 barn. This limit is however reached asymptotically at higher incident energies (E > 10 eV) from cross section values higher than the values of the free gas assumption.

Using the GA/ENDF model and a more adequate choice in the α and β grid yields a value of 20.76 barn for the scattering cross section.

The effective temperatures and Debye-Waller integrals for H in H_2O are given Table 4.1 in the section before. The IKE model results in lower values for T_{eff} compared to the GA model used in ENDF/B. This can be seen also for the average kinetic energy for H in H_2O shown in Figure 4.6 together with experimental data [16] [17].

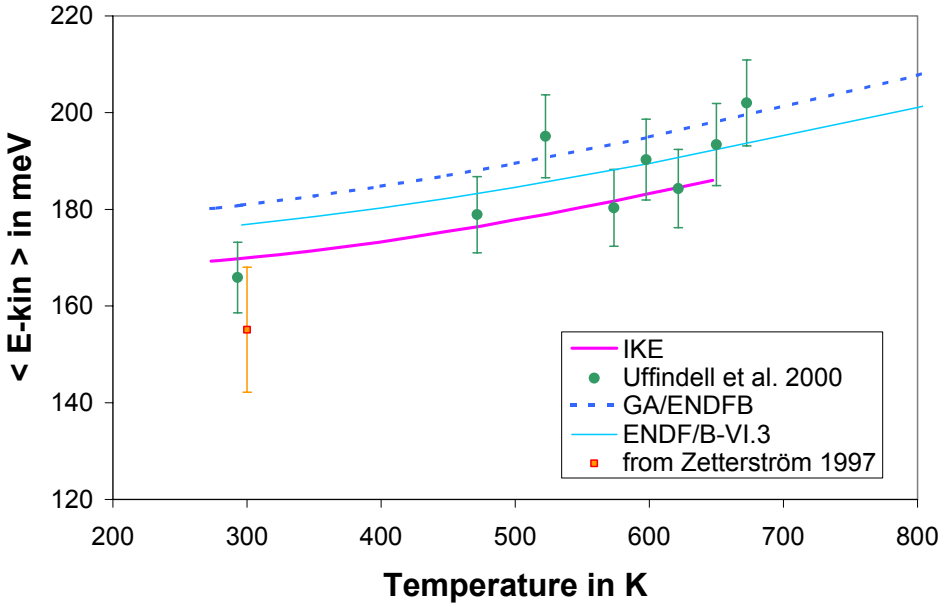

Figure 4.6 Average kinetic energy of H bound in liquid water

As in the coding of the LEAPR module one component for T_{eff} is missing (*translational part not included in the output to the ENDF file*), the results differ for the ENDF/B-VI.3 data compared to the original GA values. LEAPR was updated at IKE for the correct weighting of the modes contributing to T_{eff}.

4.3 Neutron Scattering Cross Sections

Using the THERMR module of NJOY the total scattering cross section can be calculated from the evaluated S(α,β) as well as secondary neutron distributions for a fix grid of incident energies (given in a data statement in THERMR). Examples of secondary neutron spectra are given in Figure 4.7.

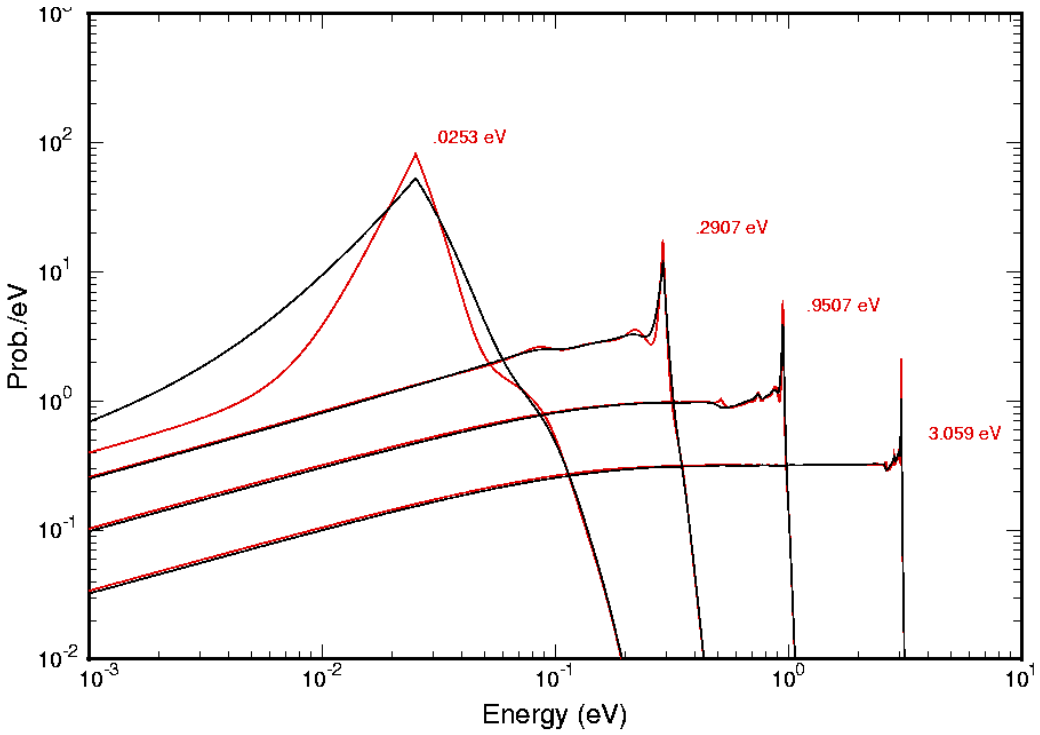

Figure 4.7 Secondary neutron spectra for H in H_2O for several incident neutron energies at a temperature of 293.6 K (red curve IKE) compared to ENDF/B-VI data (black curve)

In THERMR it is not possible to have as input discrete incident or secondary neutron energies or scattering angles nor to calculate directly values for the H_2O molecule, that means to add directly the free gas value for oxygen.

For the validation and verification of the generated thermal scattering data calculations of differential and double-differential cross sections at specific incident and secondary energies as well as at specific scattering angles of the experiments are necessary. For these purposes codes have been written specifically.

For energy transfer higher than β_{max} the short collision time approximation is used in THERMR.

4.4 Validation of Differential Neutron Scattering Cross Sections

The following figures show measured double-differential neutron scattering cross sections of light water H_2O [18] for three different incident neutron energies (154, 231 and 631 meV) at an scattering angle of 60° together with calculated ones based on S(α,β) from the IKE model as well as those derived from the ENDF/B-VI.3 data.
Good agreement and an improvement over the ENDF/B-VI data can be seen at least for the two lowest incident energies.

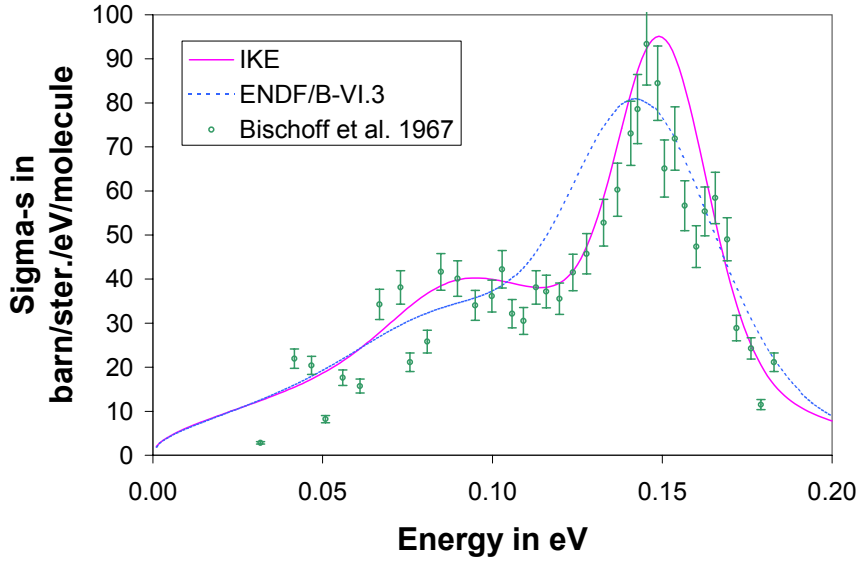

Figure 4.8 Double differential neutron scattering cross section of water around room temperature (E_i = 154 meV, θ=60°)

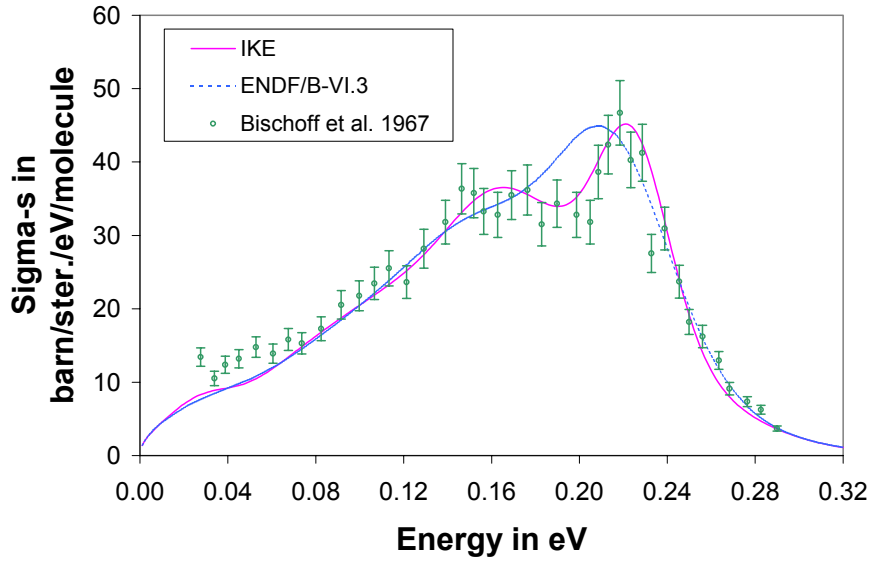

Figure 4.9 Double differential neutron scattering cross section of water around room temperature (E_i = 231 meV, θ=60°)

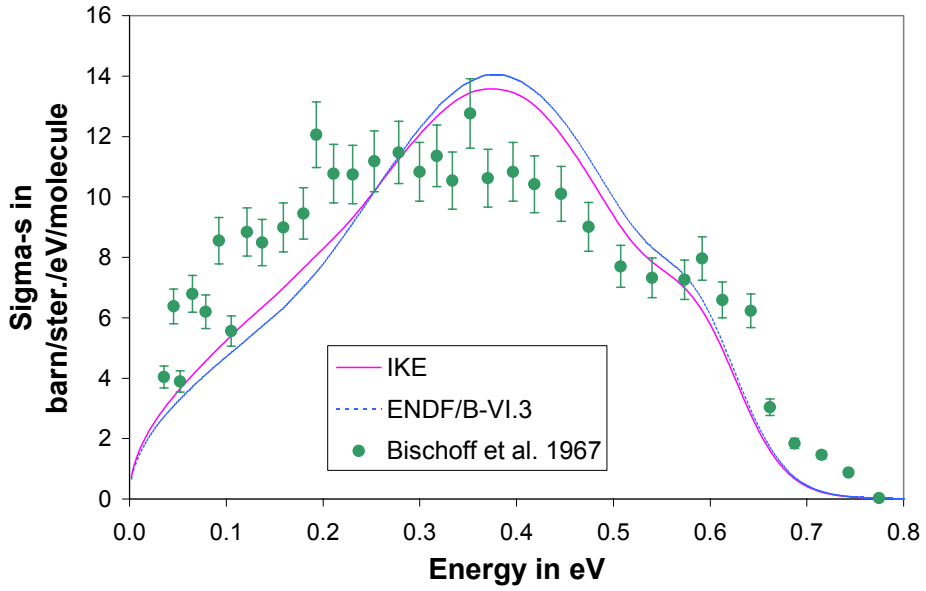

Figure 4.10 Double differential neutron scattering cross section of water around room temperature (E_i = 631 meV, θ=60°)

In Figure 4.11 up to Figure 4.14 angular distributions of neutrons scattered in H_2O are represented for several incident neutron energies (9.1, 25.3, 56.9 and 114 meV) near room temperature compared with experimental data of Beyster [20].

.

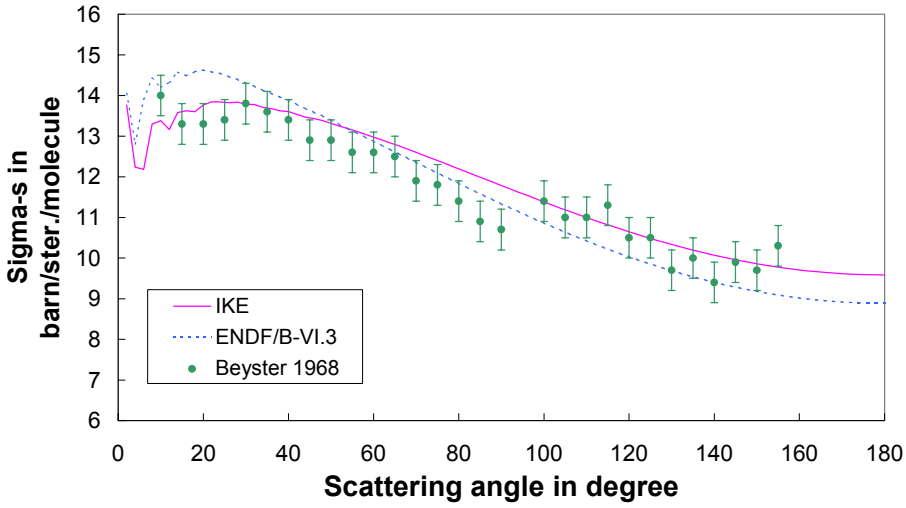

Figure 4.11 Differential neutron scattering cross section of water around room temperature (E_i = 9.1 meV)

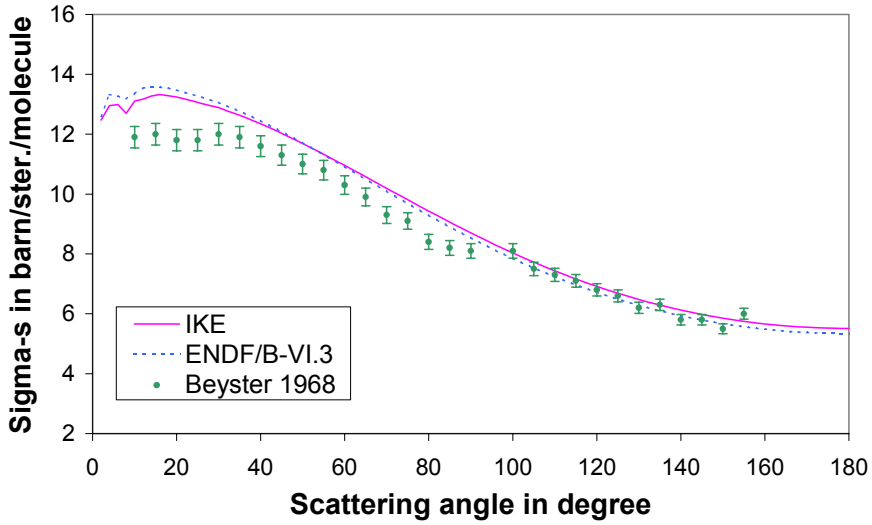

Figure 4.12 Differential neutron scattering cross section of water around room temperature (E_i = 25.3 meV)

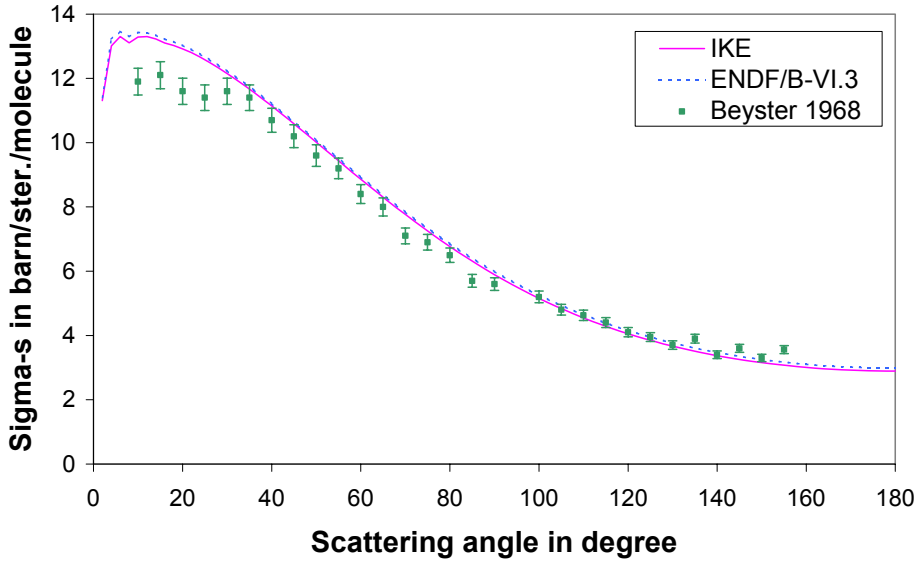

Figure 4.13 Differential neutron scattering cross section of water around room temperature (E_i = 56.9 meV)

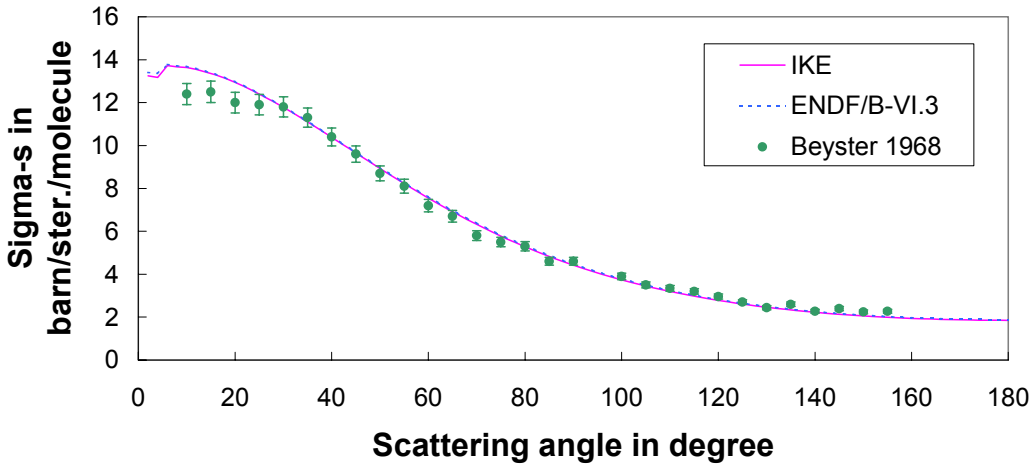

Figure 4.14 Differential neutron scattering cross section of water around room temperature (E_i = 114 meV)

4.5 Total Neutron Cross Sections for H_2O

In the following figures the total neutron cross sections for H_2O are given for room temperature and 473 K compared to measurements found in EXFOR [21], [22], [23], [24], [25]. The neutron cross sections for oxygen in free gas approximation are taken from ENDF/B-VI.

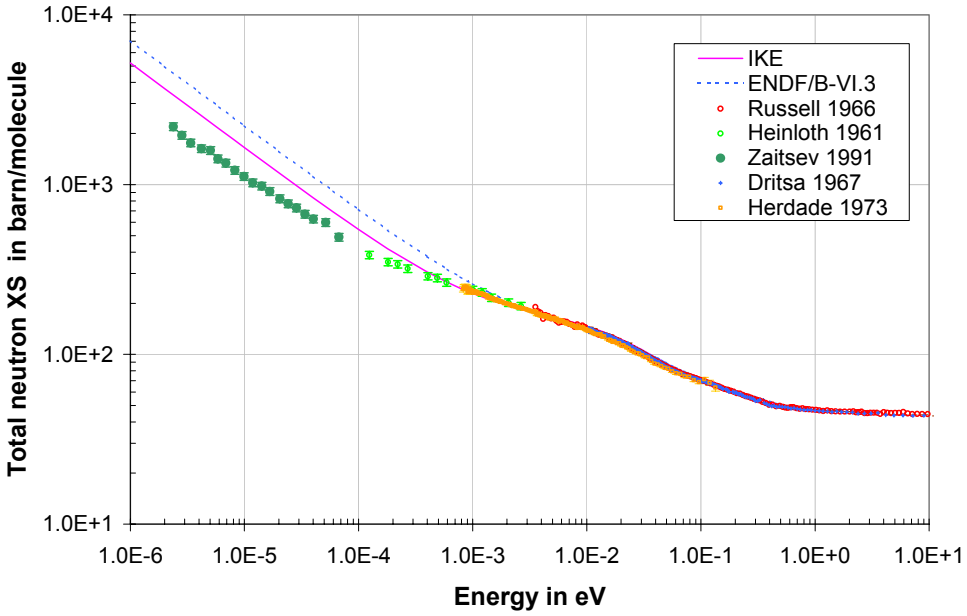

Figure 4.15 Total cross section for light water around room temperature for ultracold, cold and thermal neutrons (0.000001 up to 10 eV)

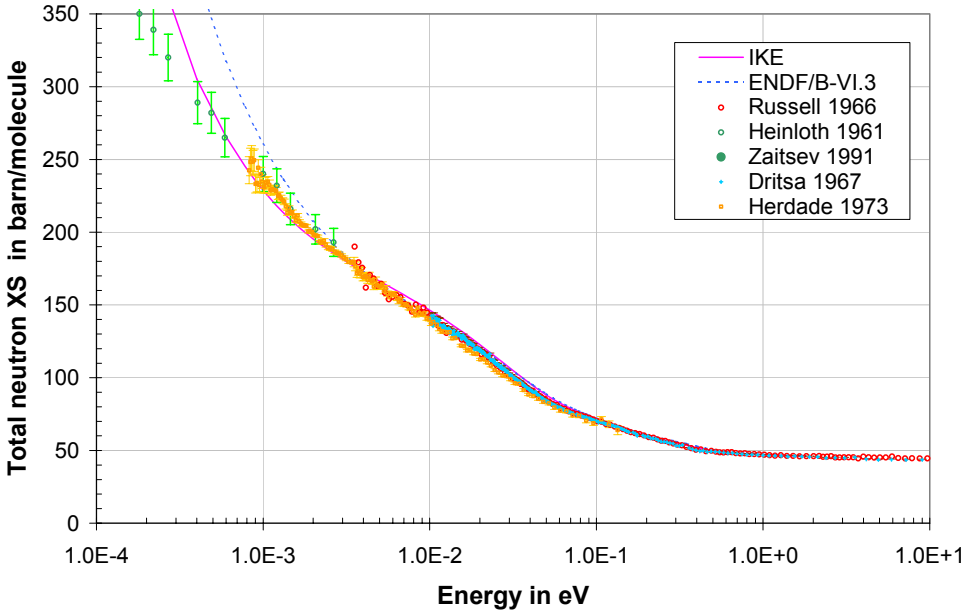

Figure 4.16 Total neutron cross section for light water around room temperature (linear scale)

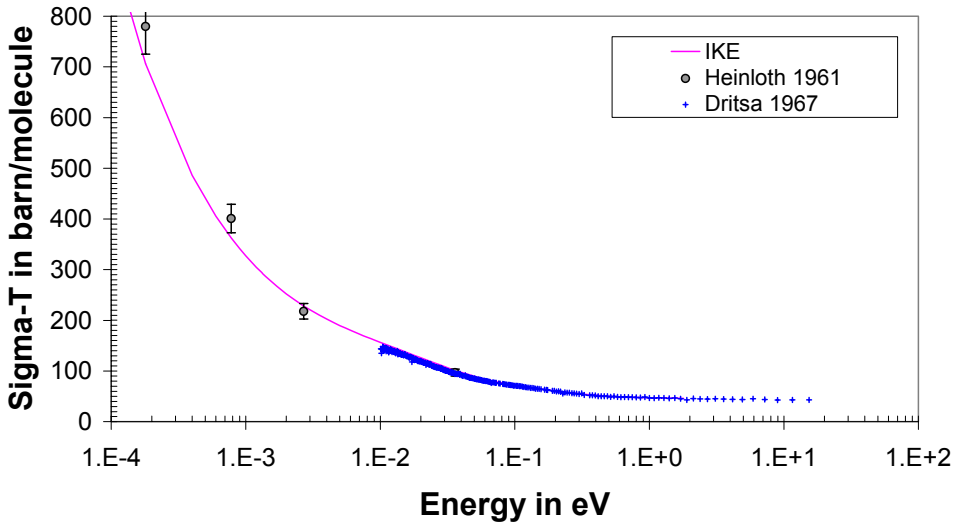

Figure 4.17 Total neutron cross section for light water at 473 K

The temperature dependence of the scattering cross section of H bound in H_2O is shown in Figure 4.18.

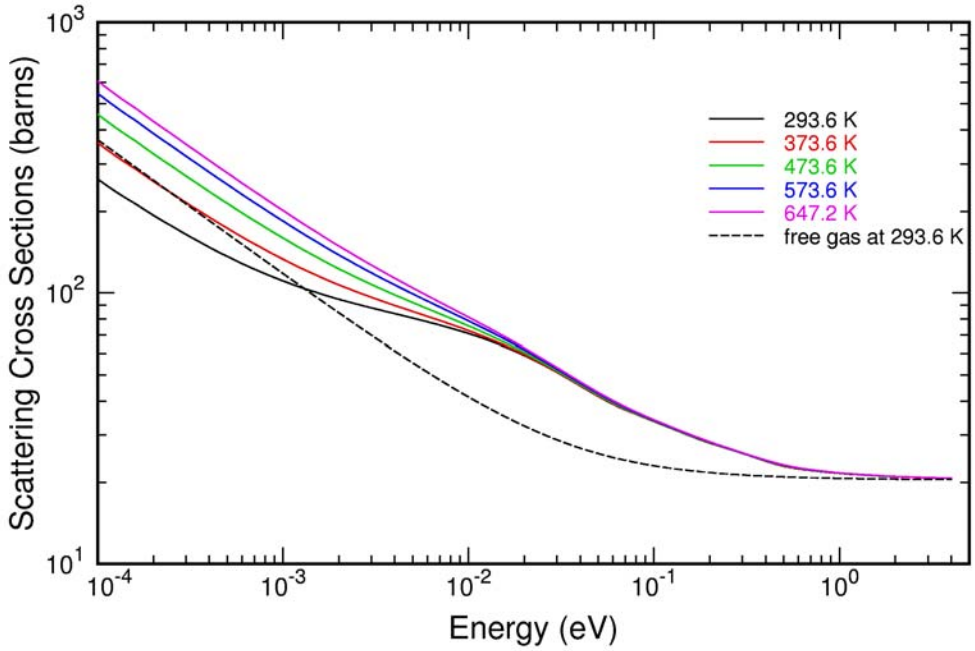

Figure 4.18 Neutron scattering cross section for H bound in H_2O at several temperatures together with the free-gas approximation for H at RT.

4.6 Average Cosine of the Neutron Scattering Angle in Water

Calculated results for the water molecule are compared with measurements from [26], [27], [20] in Figure 4.19 and Figure 4.20.

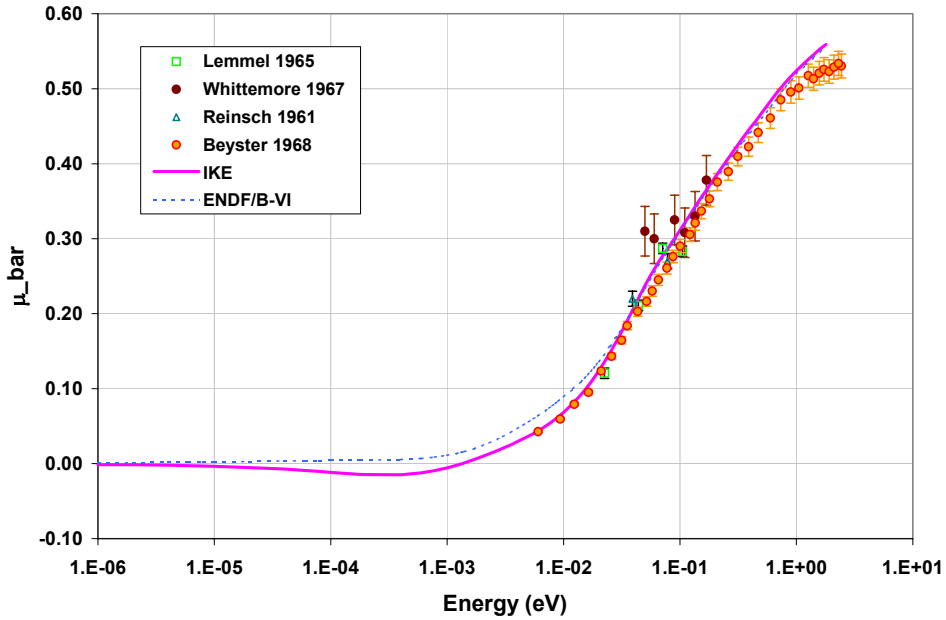

Figure 4.19 Average cosine of the neutron scattering angle for H2O around room temperature

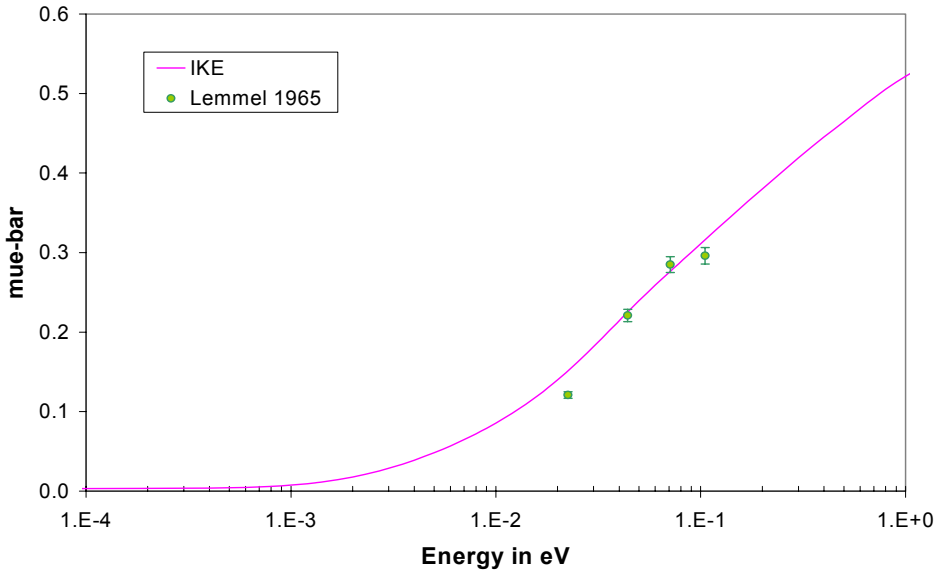

Figure 4.20 Average cosine of the neutron scattering angle in light water at 473 K

4.7 Neutron Flux Density Spectrum in H_2O

MCNP data sets in ACE format based on the IKE model were generated with NJOY using the modules THERMR and ACER for 16 angles and 64 equally energy bins for the secondary energies. For the verification of the data neutron flux density spectra in H_2O were calculated by MCNP-4C3 and MCNPX and compared with experiments. As an example Figure 4.21 shows the results for pure light water at room temperature. The measured values are taken from [28]

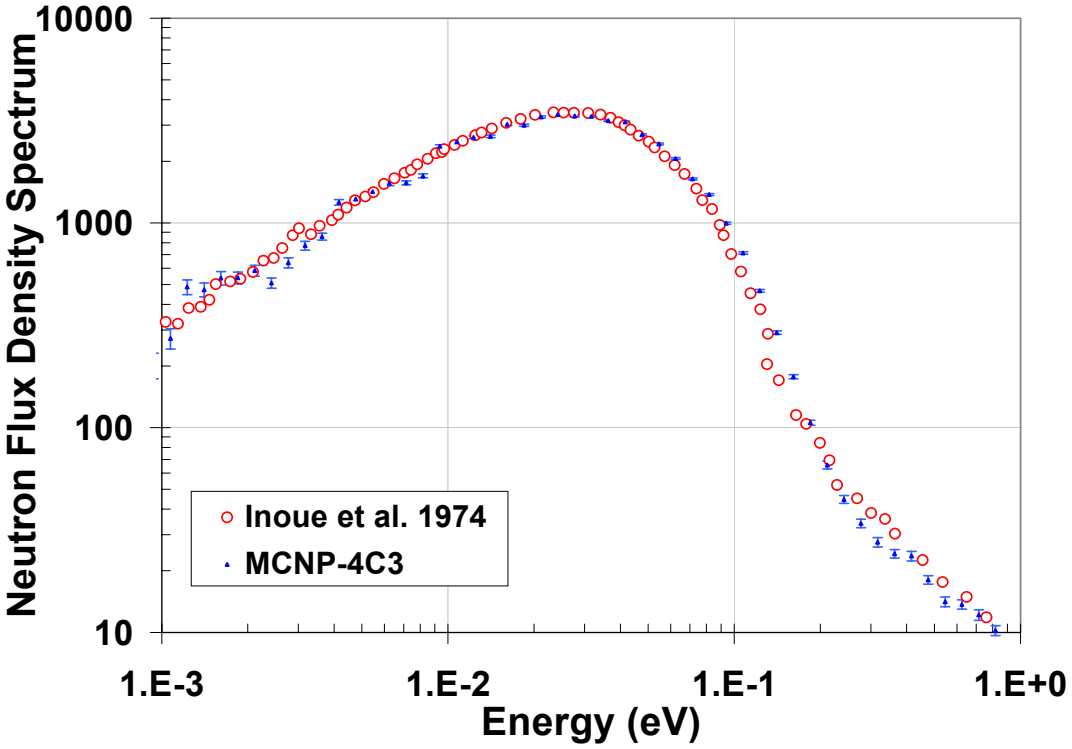

Figure 4.21 Neutron flux density spectrum of light water at room temperature

5 Zirconium Hydride

5.1 General Remarks

This evaluation for scattering law data for H in ZrH_x (variable stoichiometry with $x \leq 2$) is based on former work on metal hydrides in fcc lattice structure done at IKE [29] [30] using the code PHONON (developed at IKE) in addition to the code GASKET. The basis for PHONON was the so-called phonon expansion method as used in LEAPR to generate Scattering Law data.

No changes have been made in the physics for the generalised frequency distribution $\rho(\omega)$. For the input to LEAPR an equidistant grid for $\rho(\omega)$ was built and the α and β grid is strongly associated to the maximal and minima of the frequency spectra and its multi-phonon excitations. The α range is extended to small values.

Compared to the ENDF model from Slaggie [31] for H in ZrH_x and Zr in ZrH_x the overall agreement of measured data and calculated cross sections based on the IKE model for H in ZrH_x and treating Zr as free gas is as good or better.

5.2 Physical basis of thermal neutron interaction in zirconium hydride

The thermal neutron interaction in zirconium hydride is strongly influenced by the bound hydrogen in the lattice. As is known from the phase diagram under normal conditions zirconium hydride has several lattice structures dependent on the hydrogen content. At low hydrogen concentrations the lattice structure is a mix of hexagonal lattice (α-phase) and face centred cubic (fcc) lattice structure (δ-phase). At medium concentrations as for ZrH_x with x around 1.5 we have a pure fcc lattice for the hydride. For greater values of x a mix of fcc and face centred tetragonal (fct) hydride exists. For x around 2 we have the pure fct ε-phase. X equal 2 is the maximal possible value for zirconium hydride.

For the δ- and ε-phases the zirconium hydride lattice can be approximately represented by the main lattice of fcc metal atoms. The hydrogen atoms form a primitive cubic sub-lattice, so that the hydrogen atom is centred in a tetrahedron of surrounding metal atoms. At room temperature the distance between Zr and H is 2.07 Å, whereas the distance of neighboured H is 2.39 Å. From this structure the bound proton has an isotropic harmonic potential. Therefore the optical mode excitation can be well be described by a harmonic Einstein δ-oscillator. From known force constants an optical peak around 137 meV can be derived. As the H-H interacting forces are neglected, no splitting of the peak structure will be seen.

The generalized frequency spectra for H bound in zirconium hydride is composed of

- acoustical modes with a Debye Ansatz and a Debye temperature of 20 meV
- an optical branch approximated by a Gaussian Peak with a FWHM of 28 meV (full width of half maximum).

The ratio of the optical branch to the acoustical one is 240:1 which is taken over from the study of Slaggie [31] based on a central force dynamical calculation of the fcc zirconium hydride lattice. From the derived dispersion relations frequency distributions are calculated for the molecule as well as for the metal and hydrogen components. The consideration of the H-H interaction yields a splitting up of the optical peak for hydrogen. As shown in

comparisons with measured double differential neutron scattering cross sections, this splitting up is overestimated (see Figure 5.3 up to Figure 5.6).

The frequency distribution of the IKE model is presented in Figure 5.1 in comparison to the model used for the ENDF/B-VI data.

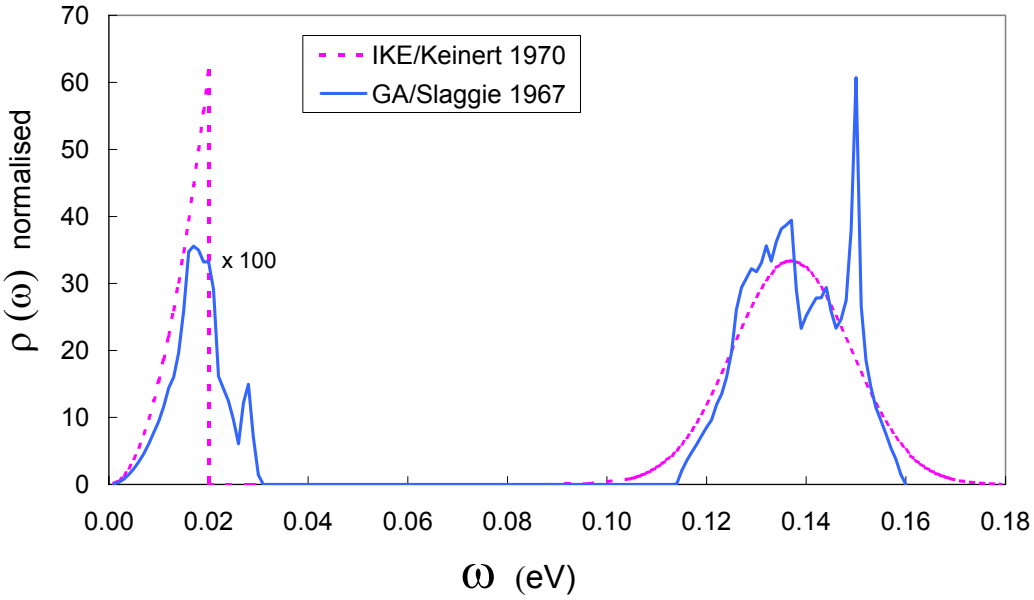

Figure 5.1 Frequency distribution of H bound in zirconium hydride

In all known models the frequency distributions ρ(ω) are handled in harmonic approximation. This means that the effects of temperature changes on the lattice structure and the force constants are not taken into account and ρ(ω) is temperature independent.

For the optical part a phonon spectrum of H in ZrH_2 published by Evans et al. [32] and based on experimental data was used to derive a complete frequency distribution with an acoustical part and weights as in the IKE model (green curve in the figure aside). For room temperature the calculated differential neutron cross sections compared to experimental data show a similar behaviour as the results based on the Slaggie model as can be seen in Figure 5.5 and Figure 5.8. The agreement with experiments and the results based on the IKE model is often better.

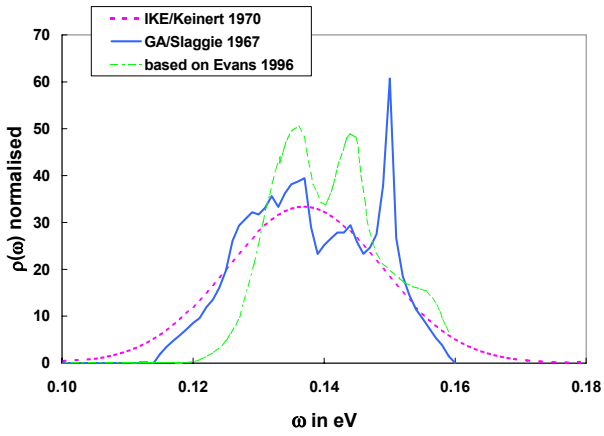

5.3 Notes to LEAPR input

The complete input to LEAPR is given in the Appendix (section10.2.2) for H in ZrH. For 8 temperatures as given in Table 5.1 scattering law data are generated for the incoherent inelastic part and the Debye-Waller integrals needed for the incoherent elastic part of thermal neutron scattering data sets in ENDF-6 format.
As an adequate choice to represent the structure of the frequency distribution as well as multiple phonon excitations 147 α values and 185 β values have been chosen for the α, β grid. The upper limit for β corresponds to E_{max} of 1.8554 eV, which is higher than the binding energy [33] of 1.04 eV for H bound in ZrH_2. This energy value decreases to 0.90 eV for $ZrH_{1.5}$. The number of principal scattering atoms in compound (*npr*) is set to one in LEAPR input.

Table 5.1 Effective Temperatures and Debye-Waller integrals for H in ZrH

Temperature K	**Effective Temperature** K	**Debye-Waller Integral** eV^{-1}
293.6	800.0	9.031
400	824.2	9.835
500	863.4	10.75
600	915.6	11.79
700	977.8	12.92
800	1047.5	14.12
1000	1202.5	16.67
1200	1370.8	19.34

The new evaluation was run through the THERMR module of NJOY to obtain integrated cross sections. Figure 5.2 shows the total and the partial neutron scattering cross sections for H in ZrH at room temperature and 1000 K.

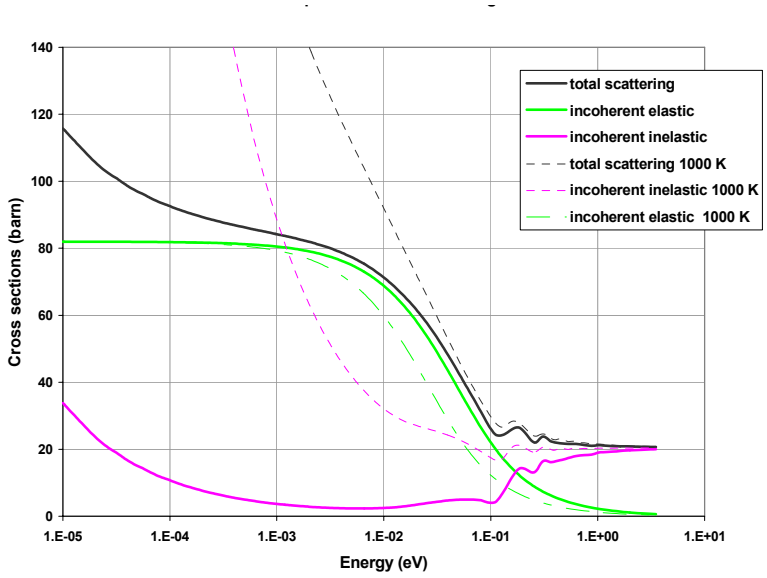

Figure 5.2 Neutron scattering cross sections for H in ZrH at 293.6 K and 1000 K

5.4 Validation of the Generated Scattering Law Data Files for H in ZrH

From the generated neutron scattering data files in MF=7 for the inelastic incoherent part (MT=4 with S(α,β)) and the incoherent elastic part (MT=2) differential and integral neutron cross sections are calculated and compared with experiments. Zr was considered in free gas approximation. Treating Zr as in the GA model Zr(ZrH) showed no differences.

5.4.1 Double Differential Neutron Cross Sections

The structure predicted in the optical peak by the central force model of Slaggie is not confirmed by experimental data for ZrH_2 [34] as shown in the following figures for an incident energy of 238 meV and several scattering angles.

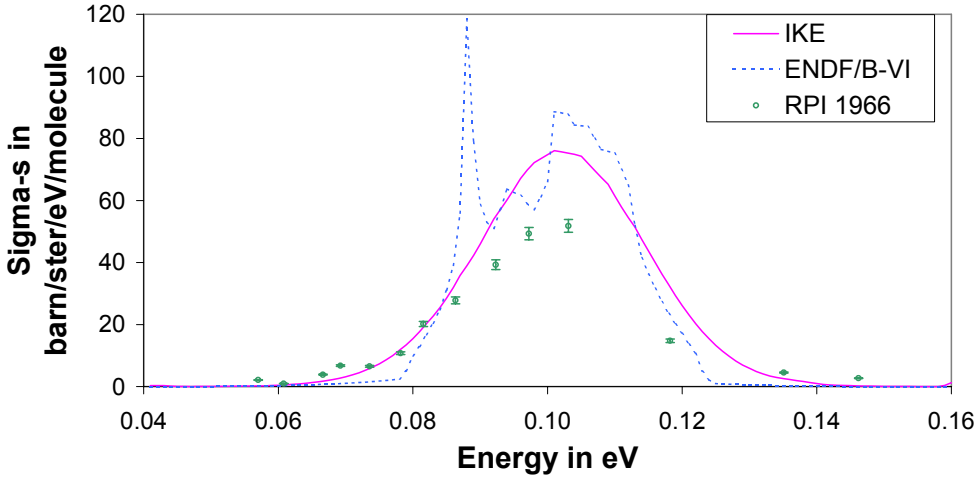

Figure 5.3 Double-differential neutron scattering cross section of ZrH_2 (E_i=238 meV, θ=25°, RT)

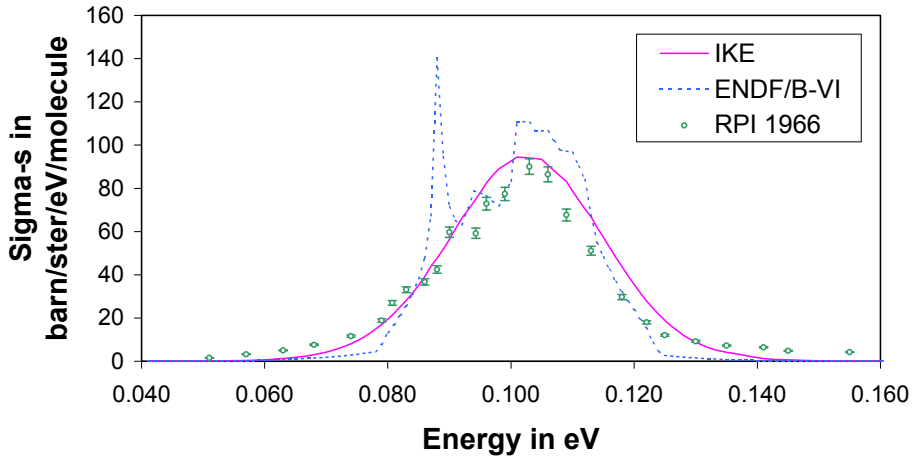

Figure 5.4 Double-differential neutron scattering cross section of ZrH_2 (E_i=238 meV, θ=40°, RT)

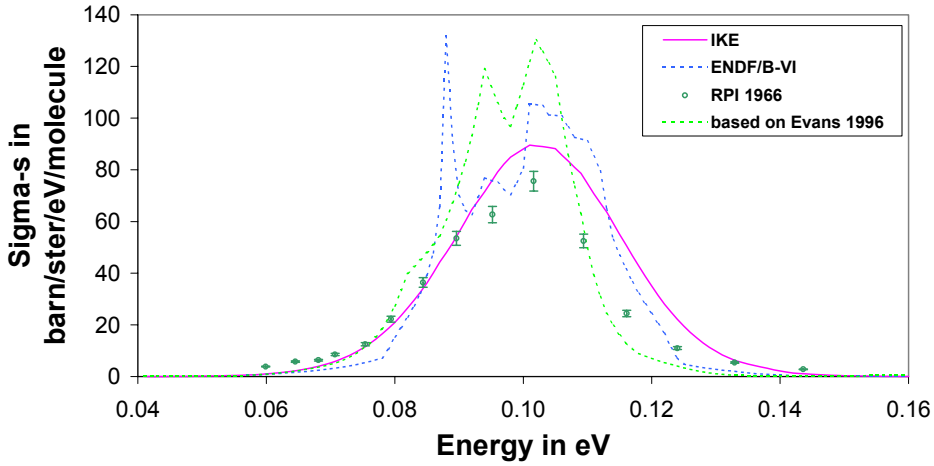

Figure 5.5 Double-differential neutron scattering cross section of ZrH_2 (E_i=238 meV, θ=60°, RT)

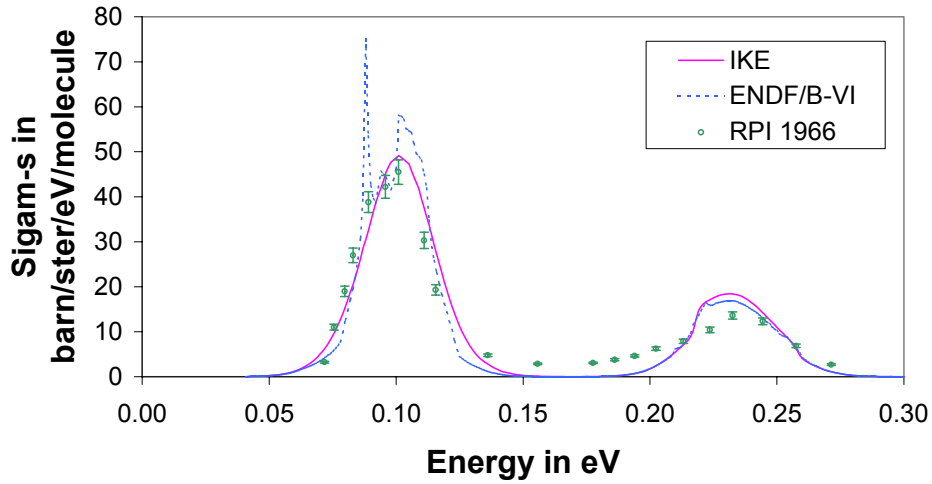

Figure 5.6 Double-differential neutron scattering cross section of ZrH_2 (E_i=238 meV, θ=90°, RT)

Double-differential neutron scattering cross of ZrH_2 at an incident energy of 572 meV for several scattering angles are given in the following figures based on the IKE model as well as generated from the ENDF/B-VI.3 data in comparison with measurements done at RPI [35] around room temperature RT.

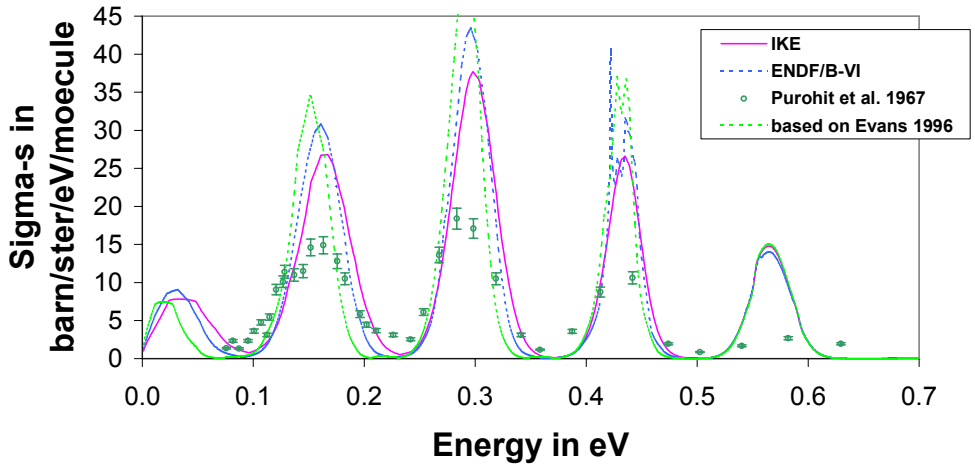

Figure 5.8 Double-differential neutron scattering cross section of ZrH_2 (E_i=572 meV, θ=60°, RT)

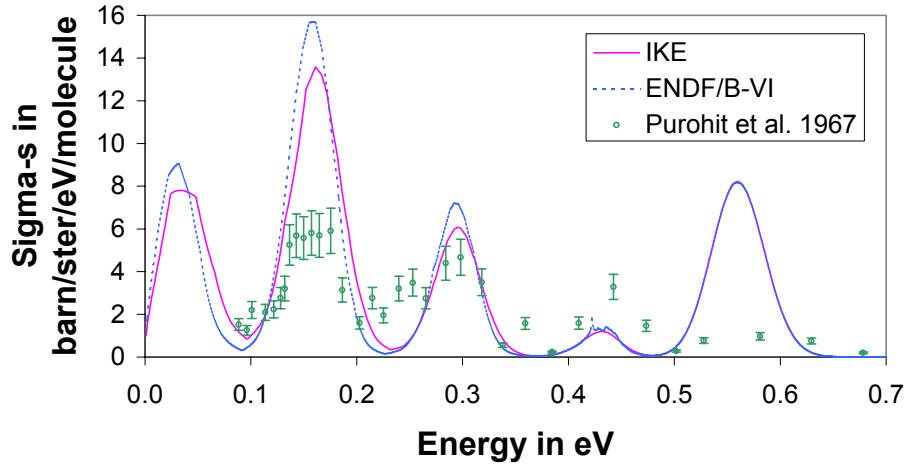

Figure 5.9 Double-differential neutron scattering cross section of ZrH_2 (E_i=572 meV, θ=90°, RT)

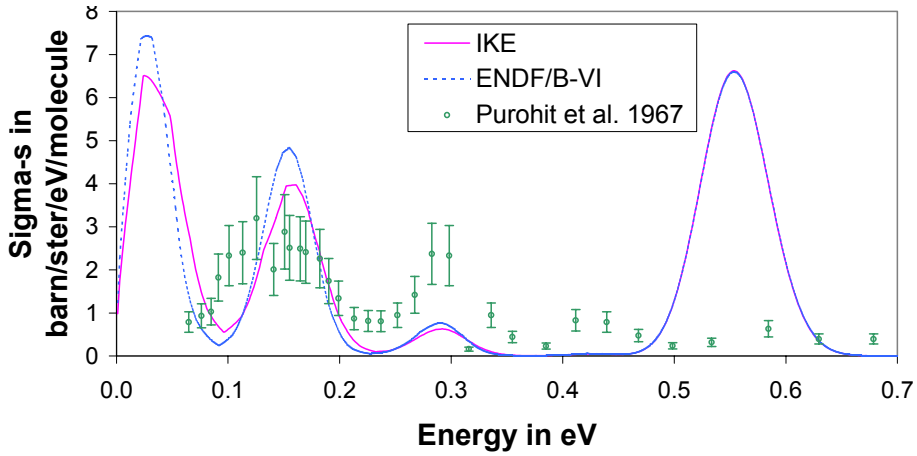

Figure 5.10 Double-differential neutron scattering cross section of ZrH_2 (E_i=572 meV, θ=120°, RT)

5.4.2 Comparison with Measured Scattering Law Data at 483 K

For $ZrH_{1.08}$ there are available measured scattering law data $S(\alpha,\beta)$ at a temperature of 483 K

[36] for several values of β i.e. energy transfers. In Figure 5.11 these $S(\alpha,\beta)$ data are compared with the generated ones from IKE and ENDF/B at four energy transfers from 16.6 up to 158.2 meV.

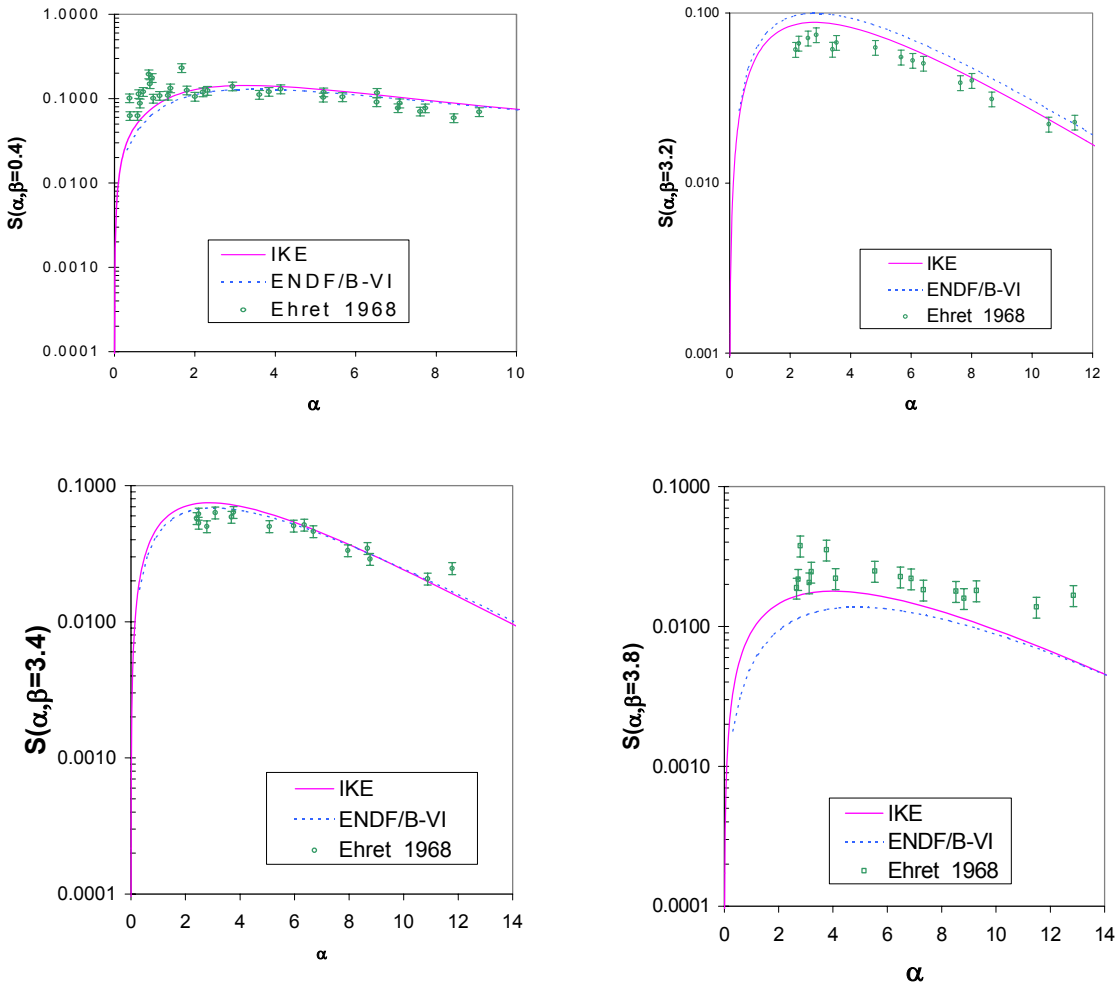

Figure 5.11 Scattering law for $ZrH_{1.08}$ at a temperature of 483 K for several energy transfers (16.6, 133.2, 141.5 and 158.2 meV)

5.4.3 Differential Neutron Scattering for $ZrH_{1.85}$ and $ZrH_{1.92}$

For zirconium hydride $ZrH_{1.85}$ and $ZrH_{1.92}$ there are measured data by Carriveau [37] and Kornbichler [38] for differential neutron scattering cross sections as a function of the scattering angles for several incident energies. As there is an agreement between the new data (IKE) and ENDF/B compared to the experimental data only the following two figures are shown.

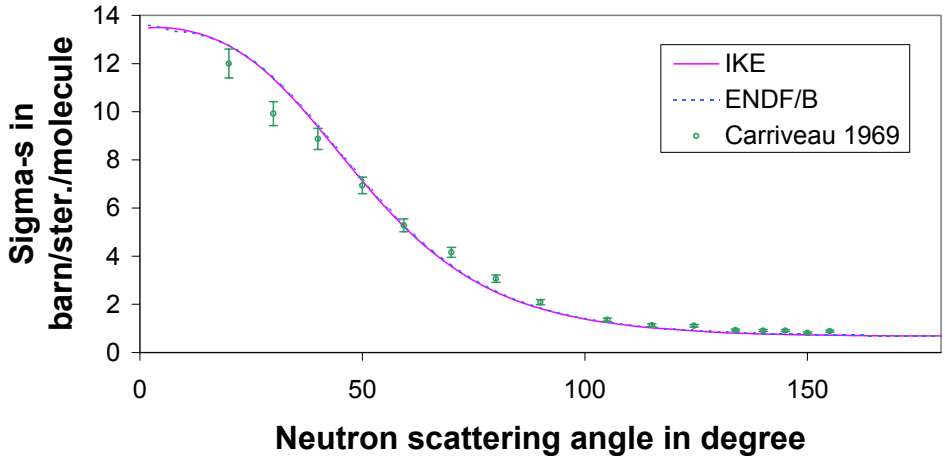

Figure 5.12 Differential neutron scattering cross sections around room temperature of $ZrH_{1.85}$ for E_i=0.8824 eV

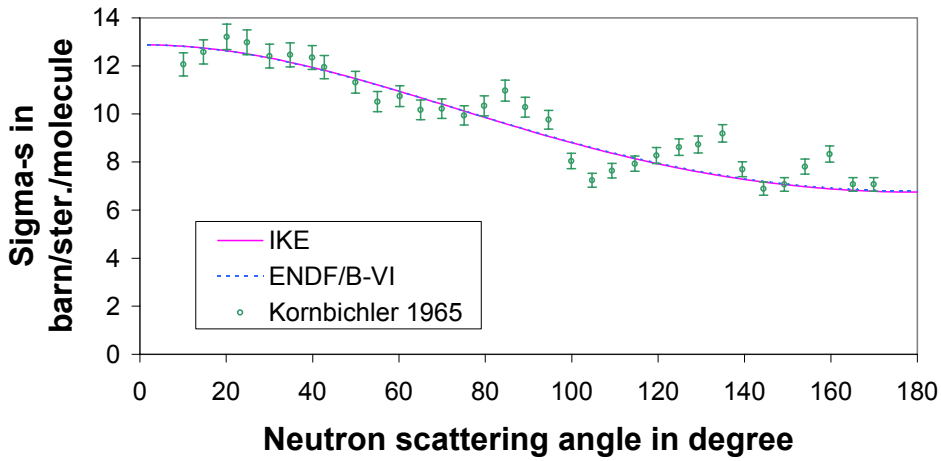

Figure 5.13 Differential neutron scattering cross sections around room temperature of $ZrH_{1.92}$ for E_i=22.5 meV

The experimental data given in Figure 5.13 show some interference structure which may be assigned to the metal component in the lattice. As the neutron scattering on Zr is treated in free gas approximation, no coherent elastic scattering is considered in the IKE model. In the ENDF model only incoherent elastic scattering is included for Zr.

5.4.4 Neutron Scattering Cross Section for ZrH

The neutron scattering cross section for H in ZrH is calculated as the sum of the incoherent inelastic cross section from S(α,β) (MT=4) and the incoherent elastic cross section (MT=2). For the scattering cross section of ZrH (shown in Figure 5.14) the contribution for Zr is treated in free gas approximation. Experimental data are from [39].

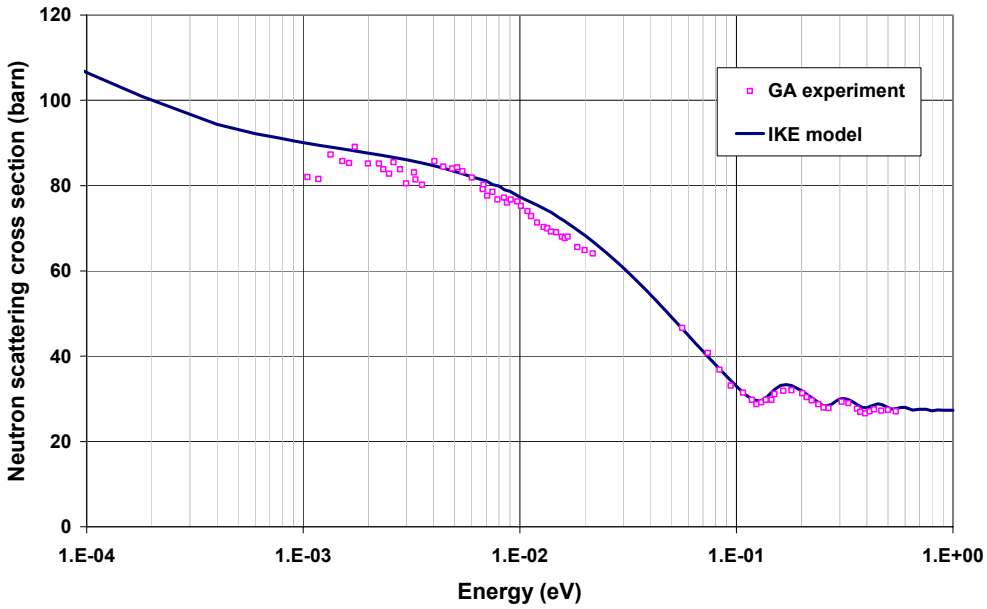

Figure 5.14 Total neutron scattering cross section for ZrH at room temperature

However for ZrH as a solid there should be a coherent elastic part. From the structure of the experimental data in the low energy range this could be expected. Therefore the coherent

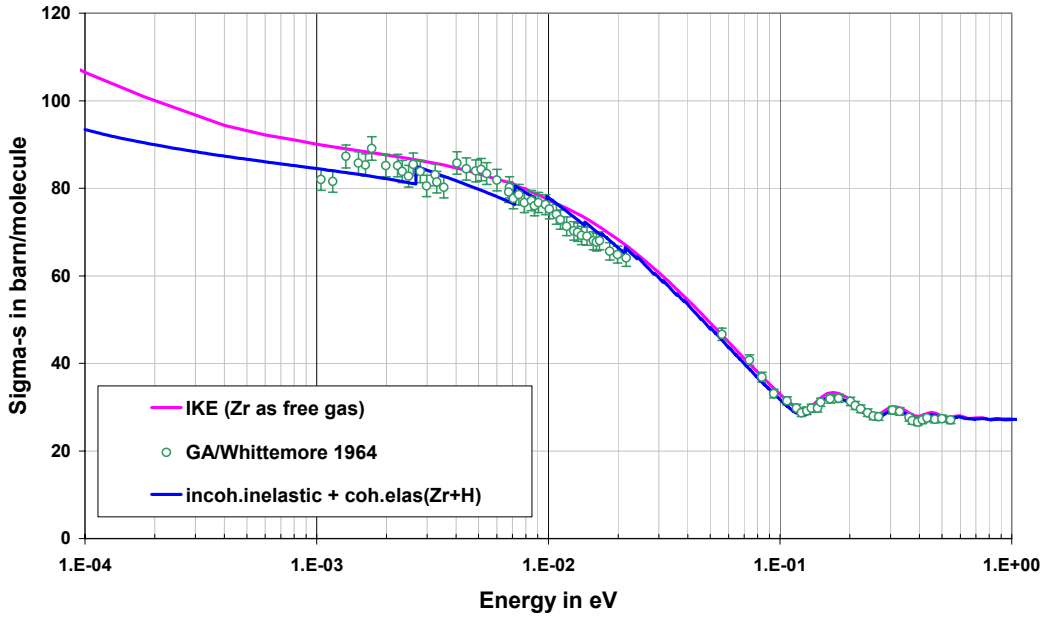

Figure 5.15 Coherent elastic scattering included in the total neutron scattering cross section in ZrH

elastic scattering was calculated for an assumed fcc lattice structure of ZrH_2 and stored in MF=7 and MT=2 instead of the original data in the file for Zr in ZrH_x of ENDF/B. The effect is clearly seen in Figure 5.15.
Due to the different stoichiometry and lattice structures of ZrH and ZrH_2 this is a first approximation to consider the coherent elastic cross section and is not universally valid. The effect is seen only for low energies less 5 meV.

Figure 5.16 represents the total scattering cross section for the n-p interaction in ZrH_x at room temperature in the energy range from 0.1 eV up to 1 eV where two measurements are available [40], [41]. A better agreement with the experimental data and the calculated ones (IKE or ENDF/B) could be achieved when additional energy points were introduced into the energy grid built into THERMR. In Figure 5.17 the calculated average cosine of the scattering angle is compared with measurements.

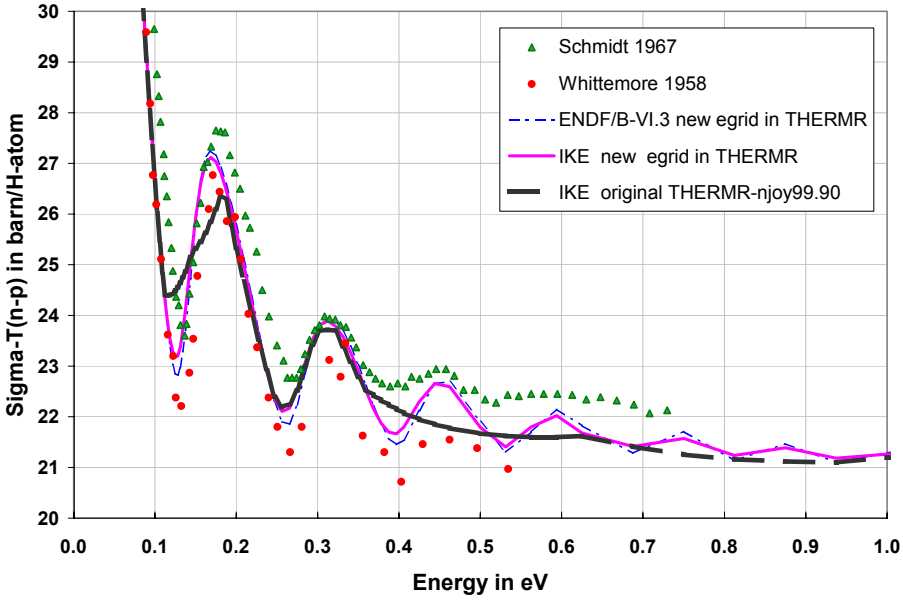

Figure 5.16 Total neutron scattering cross section of n-p interaction in ZrH_x at RT

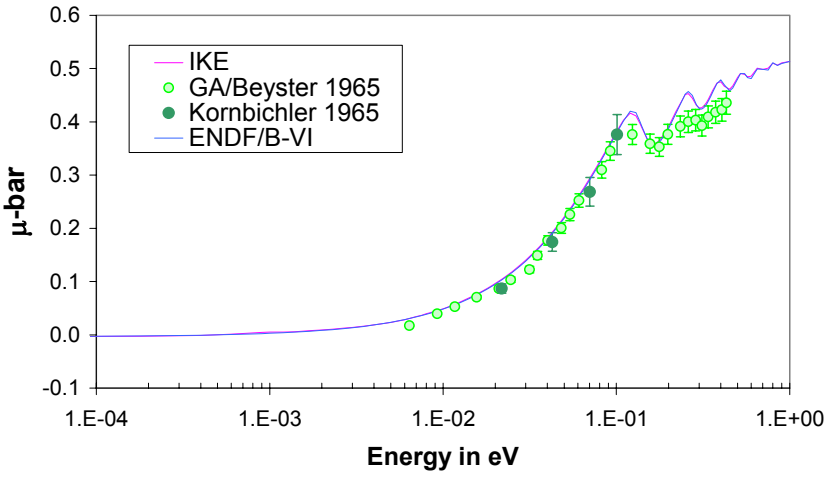

Figure 5.17 Average cosine of the scattering angle in ZrH_x (x ≈1.84) at RT

5.5 Neutron flux density spectra

Measured neutron flux density spectra [42] are compared with calculations done by Bernnat/IKE [43] using the Monte Carlo code MCNPX and the generated data sets in ACE format based on the IKE evaluation for H(ZrH) (see section 7).

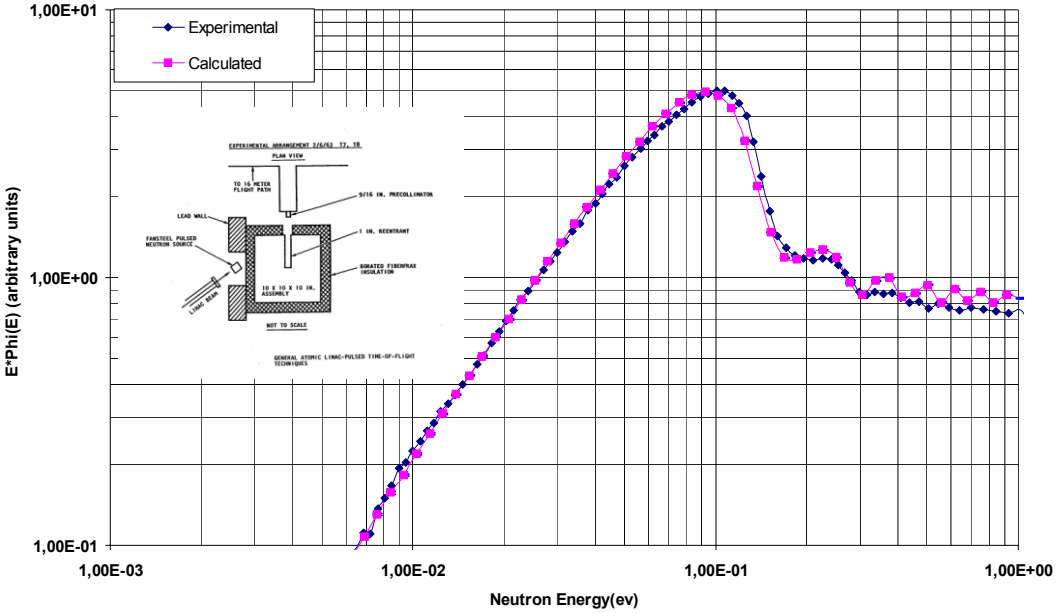

Figure 5.18 Infinite medium spectrum in borated ZrH at 295 °C, 3.4 b /H atom

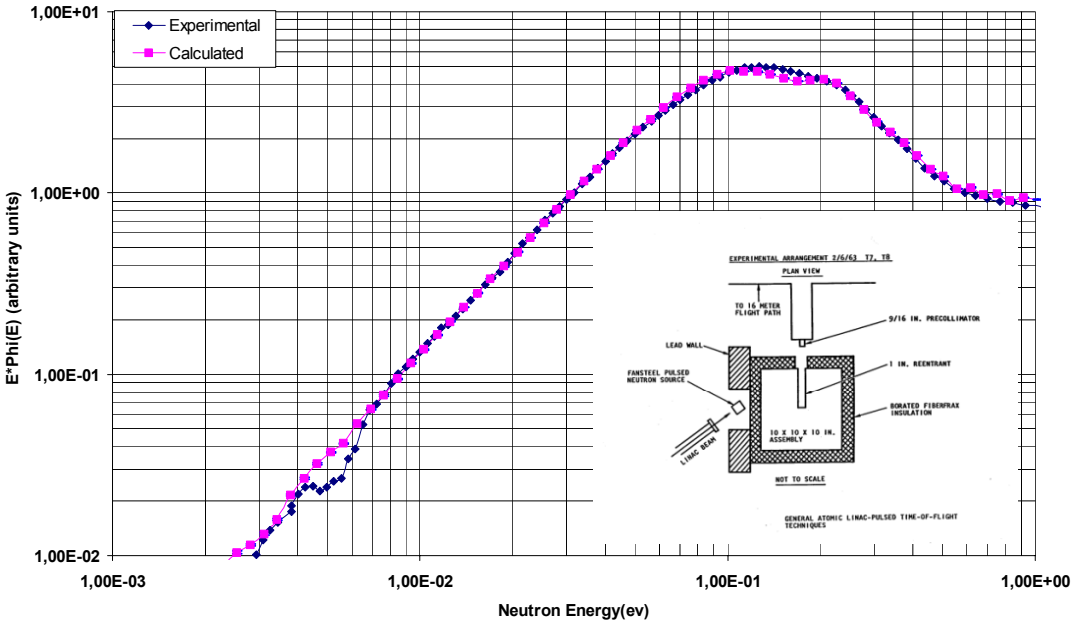

Figure 5.19 Infinite medium spectrum in borated ZrH at 468 °C, 3.4 b /H atom

6 Heavy Water, D in D_2O

The dominant coherent neutron scattering of D was never considered in the ENDF and JEF model. For the correct description of neutron scattering in D_2O the intermolecular interaction for D-D, O-D and O-O interference as well as the intra-molecular interference should be taken into account. For room temperature a study at IKE in 1992 has shown that the different intermolecular and intra-molecular contributions almost cancel out each other excluding the D-D intermolecular part.

The scattering law data for D in D_2O in incoherent approximation can be improved by consideration of the D-D intermolecular interference scattering according to the Sköld approximation. The neutron scattering on oxygen is treated as free gas.

Compared to the JEF model [6] for D in D_2O the treatment of the translational mode was modified. The α and β grid (input to LEAPR) is strongly correlated to the maxima and minima of the frequency distribution and, in addition, the α range is extended to smaller values.

6.1 The Scattering Dynamics of Deuterium bound in Heavy Water

For the dynamics of deuterium in liquid heavy water three types of motions according to the different degrees of freedom are characterising the generalised frequency distribution:

- the three acoustical modes are split into a part of hindered translations and of translational vibrations. As in our model for liquid deuterium [44] this may be discussed as a model for jump and hindered translations. The deuterium is assumed to diffuse for a certain time in the liquid and then it is localised for a certain time at a fixed place and vibrates in the condensed matter. The weight of the hindered translational mode is taken to be 0.05, which corresponds to an effective translational mass of 20. The fixed vibrational part also has a weight of 0.05 but with a Debye type distribution for a Debye temperature of 20.2 meV.

- for the three rotational degrees of freedom a broad band of frequencies is assumed according to the results of Haywood and Page [12] being dependent on temperature. For a given temperature the distribution is derived by linear interpolation. In contrary to the previous JEF model the weight W_s is slightly increased by the Debye part (see Figure 6.1).

- the three vibrational degrees of freedom are represented by three discrete Einstein δ-oscillators from which the two stretching vibrations are handled as degenerated with doubled weighting. As in the JEF model the frequencies are taken as 145 and 338 meV. The weight of these modes is assumed to be 0.5.

This generalised frequency distribution was taken to generate in a first step $S(\alpha,\beta)$ data in incoherent approximation by the LEAPR module. As deuterium is a dominant coherent neutron scatterer, an improvement of the scattering law data for D in D_2O could be achieved

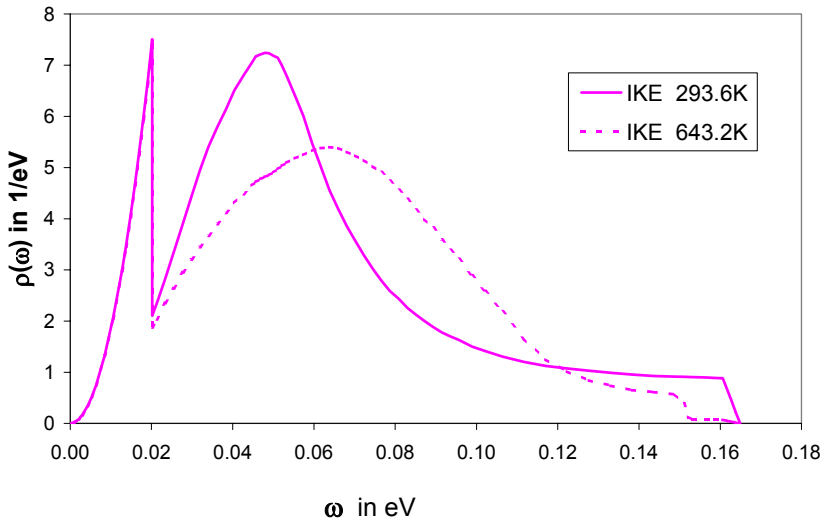

Figure 6.1 Continuous part $\rho_s(\omega)$ for the frequency spectrum for D bound in D_2O

by considering the intermolecular D-D interference. With a static structure factor S(κ) a correction of the incoherent data file according to the Sköld approximation [9]

$$S(\alpha,\beta) = \frac{\sigma^{inc}}{\sigma} S^{inc}(\alpha,\beta) + \frac{\sigma^{coh}}{\sigma} S^{inc}(\alpha',\beta)\, S(\kappa)$$

with

$$\alpha' = \frac{\alpha}{S(\kappa)} \qquad \text{and} \qquad \sigma = \sigma^{inc} + \sigma^{coh}$$

was done. The static structure factor was derived by assuming for the interacting potential for small distances a hard core model and for greater distances a Lennard-Jones potential. In Figure 6.2 the structure factors S(κ) for the two limiting temperatures 293.6 and 643.2 K are represented.

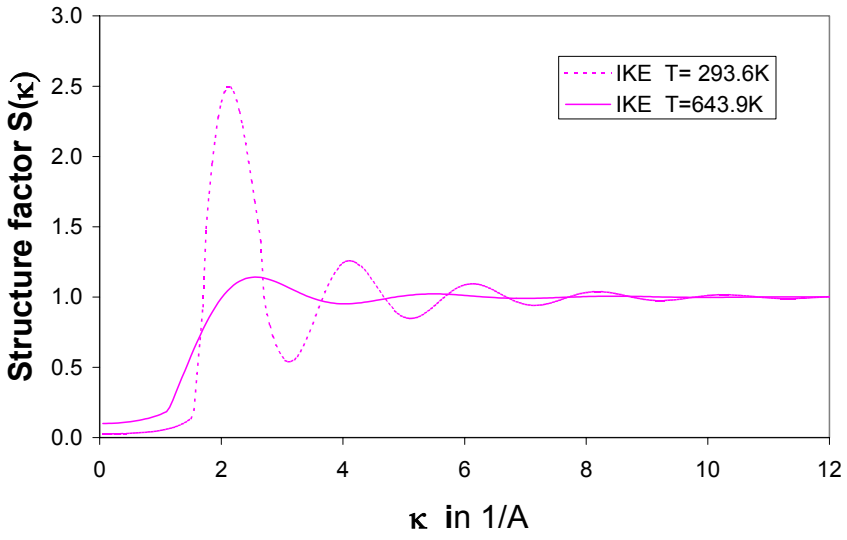

Figure 6.2 Static structure factors for intermolecular D-D interaction in liquid D_2O

These modified scattering law data with coherent contributions are stored in consistent manner in MF=7 and MT=4 of the ENDF-6 format. The further processing with THERMR is as usual. The oxygen part has to be handled in free gas approximation.

6.2 Notes to LEAPR input

The complete input to LEAPR is given in the Appendix (section 10.2.3) for D in D_2O. For 8 temperatures up to the critical temperature as given in Table 6.1 scattering law data are generated for the incoherent part of the neutron scattering. This is needed as base for the Sköld approximation to consider inter-atomic interference scattering.

As an adequate choice to represent the structure of the frequency distribution as well as all multiple phonon excitations 277 α values and 159 β values have been chosen for the α, β grid. The upper limit for β corresponds to E_{max} of 1.8554 eV, which is higher than the binding energy of 1.525 eV as given in [14]. The range for the α values is from .0001 to 146.9 and for the β values from zero to 73.334.

For each temperature of the new evaluation of $S(\alpha,\beta)$ for $D(D_2O)$ the results from LEAPR are modified as specified in Section 2.5 with the appropriate structure factor which is given in Figure 6.2 for two temperatures.

Table 6.1 Effective temperature for D in D_2O

Temperature K	**Effective Temperature** K
293.6	1010.1
323.6	1021.6
373.6	1042.3
423.6	1064.6
473.6	1088.4
523.6	1113.6
573.6	1140.1
643.9	1179.4

6.3 Validation

6.3.1 Differential Neutron Cross sections

From the generated scattering law data differential cross sections are calculated and compared with experimental results [45] [46] for several incident neutron energies as given in Figure 6.3 up to Figure 6.6. Cross sections based on S(α,β) in incoherent approximation (LEAPR) as well as cross section based on the new S(α,β) with intermolecular D-D interference are shown. The agreement of the "coherent" model is excellent.

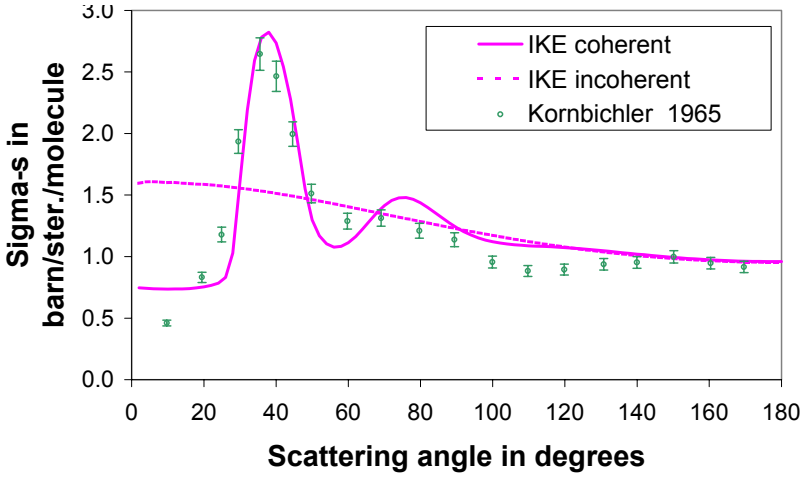

Figure 6.3 Differential neutron scattering cross section of heavy water at room temperature (E_i=22.5 meV)

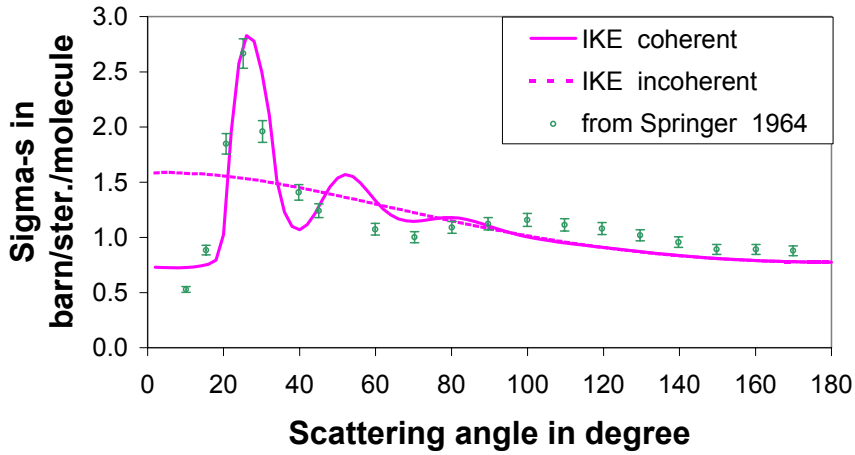

Figure 6.4 Differential neutron scattering cross section of heavy water at room temperature (E_i=44 meV)

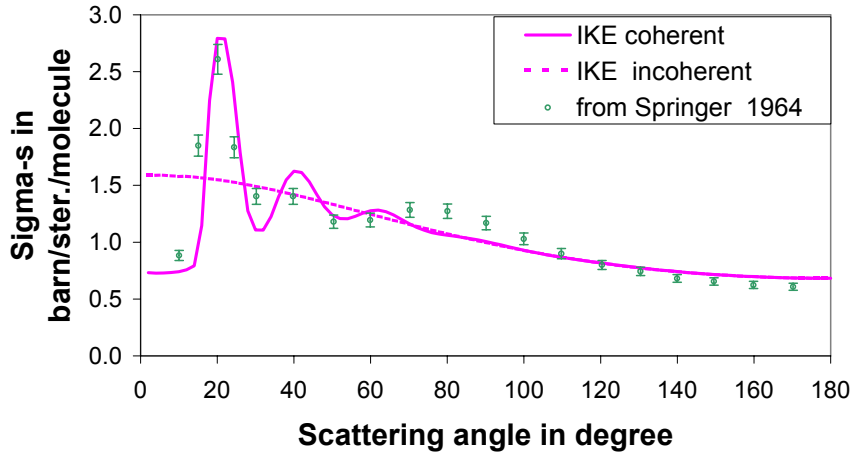

Figure 6.5 Differential neutron scattering cross section of heavy water at room temperature (E_i=71 meV)

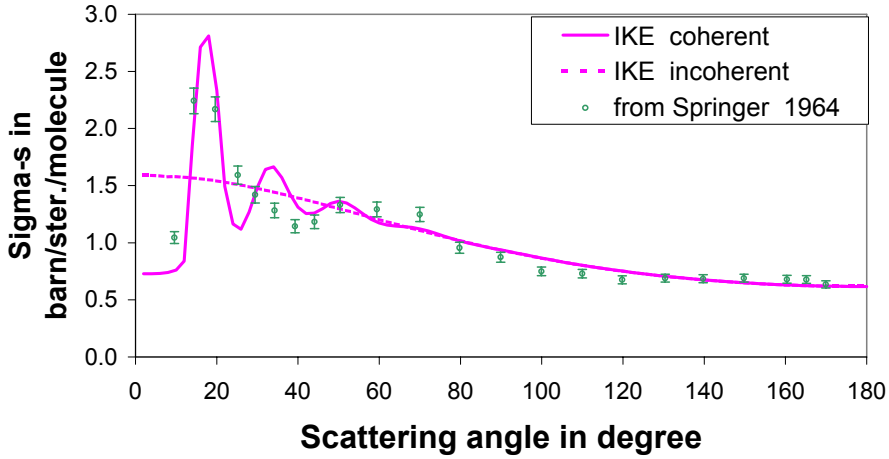

Figure 6.6 Differential neutron scattering cross section of heavy water at room temperature (E_i=105 meV)

The improvement due to consideration of interatomic D-D interference at least at smaller angles is quite evident.

In Figure 6.7 an experimental scattering law [47] is compared with the IKE and ENDF/B-VI.3 data sets. There is nearly no difference between the calculated data as the energy transfer is outside of the influence of the coherent effects.
This is valid for all greater energy transfers we have compared and therefore not given here.

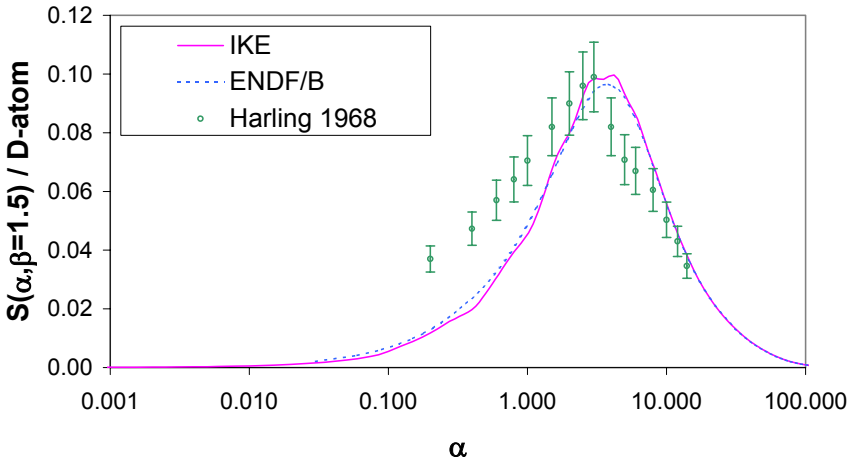

Figure 6.7 S(α,β) for heavy water with an energy transfer of 38.6 meV around room temperature

6.3.2 Total Neutron Cross Sections for D_2O

In Figure 6.8 up to Figure 6.10 the calculated total neutron cross sections for heavy water are compared with measurements given in EXFOR and data taken from [48], [23] for room temperature and at 200° C

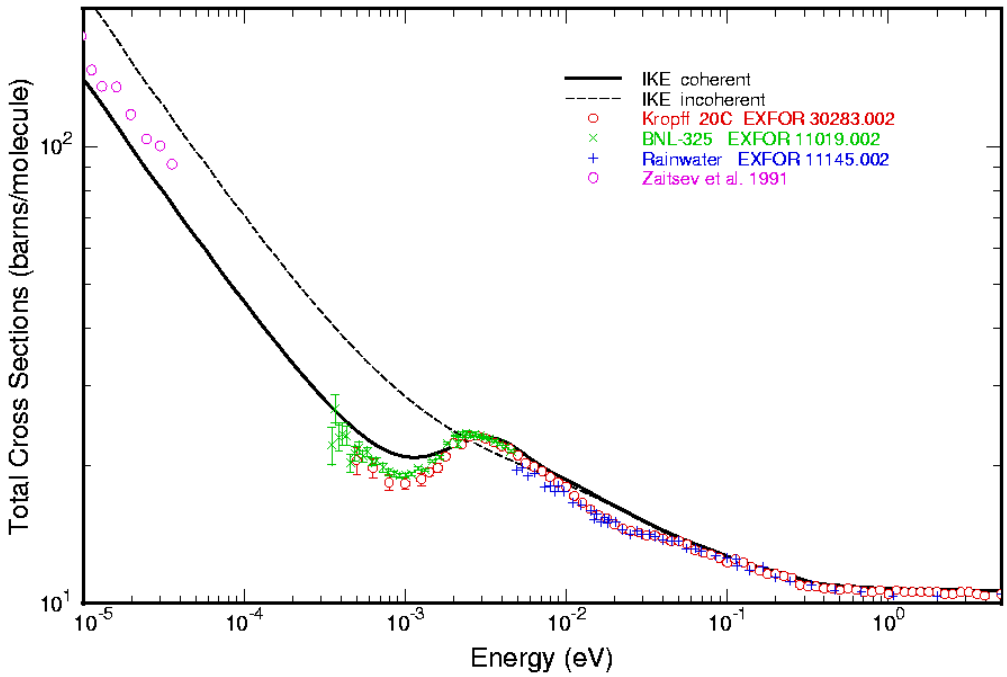

Figure 6.8 Total neutron cross section for heavy water at room temperature

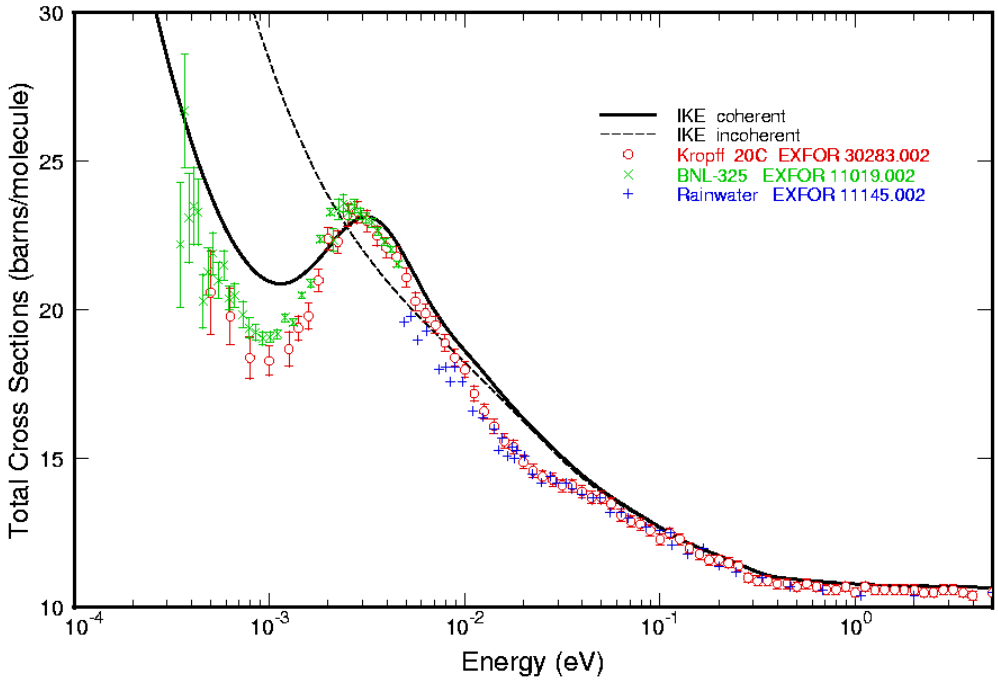

Figure 6.9 Total Neutron cross section for heavy water at room temperature

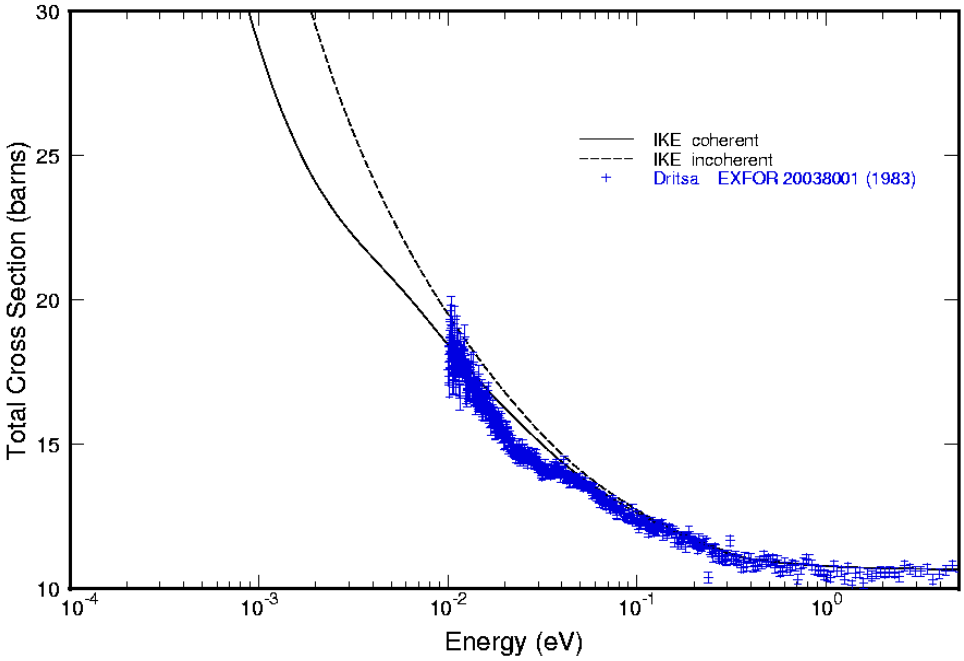

Figure 6.10 Total neutron cross section for heavy water at 200 °C

6.3.3 Average Cosine of the neutron scattering angle

Calculated results for the heavy water molecule are compared with measurements from [45] in Figure 6.11 and Figure 6.12.

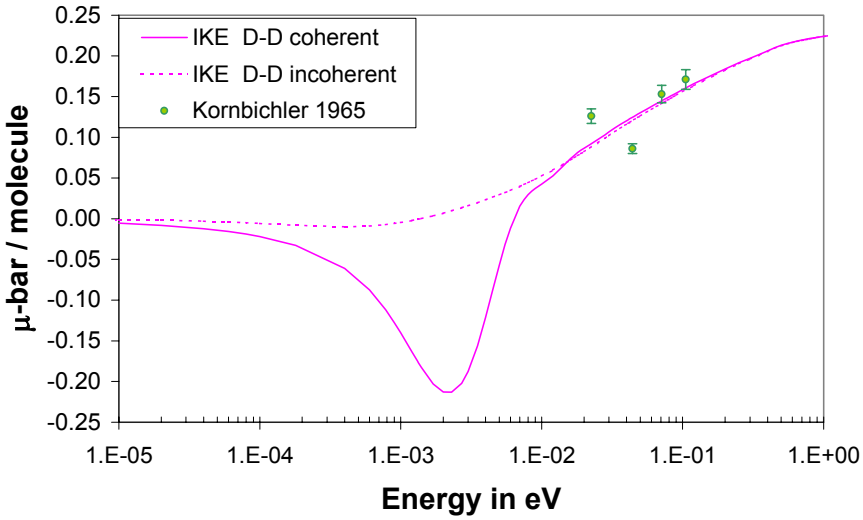

Figure 6.11 Average cosine of the neutron scattering angle in heavy water at RT

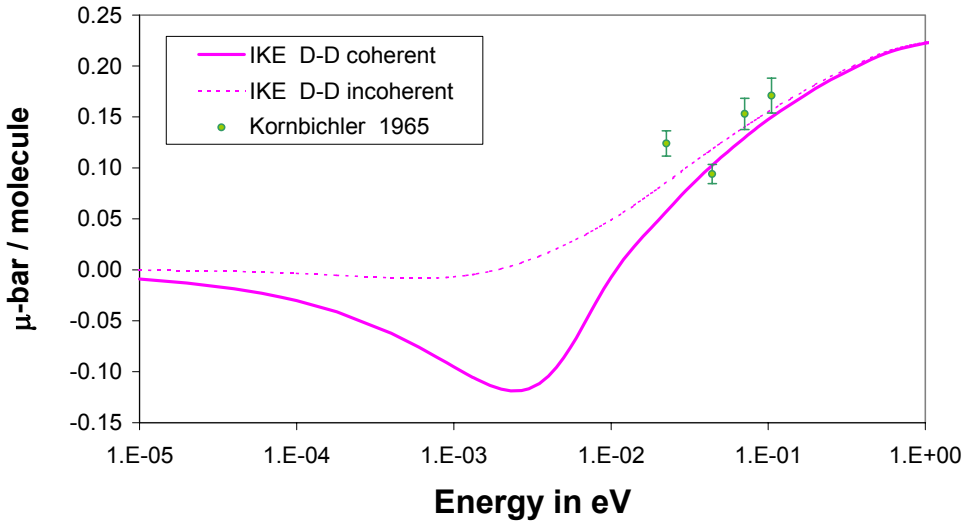

Figure 6.12 Average cosine of the neutron scattering angle in heavy water at 473 K

7 MCNP Data Sets

The NJOY processing code system was used to create S(α,β) tables for MCNP from the IAEA/IKE evaluations at a variety of temperatures. NJOY version 99.90 - with additional updates particular in the modules THERMR and ACER - was used.
The maximum incident neutron energy is 4.46 eV for H in H_2O, D in D_2O, and H in ZrH. In THERMR extra points to the energy grid for ZrH have been added to get agreement with measured neutron scattering cross sections.

A total of 27 MCNP data sets have been created for 3 moderator materials: H bound in H_2O, H in ZrH and D in D_2O. Information about these 27 data sets similar to that contained in Appendix G of the MCNP manual is provided here in the following Table 7.1. Note that these data sets may be used with any version of MCNP(X).
Given in parenthesis are the nuclides for which the S(α,β) data are valid. For example, *h2o.01t* provides scattering data only for ^{1}H; ^{16}O would still be represented by the default free-gas treatment.

Table 7.1 MCNP Data Sets in the *SAB-IKE-2004* Library

Hydrogen in Light Water H_2O (1001)						
h2o.01t	IAEA/IKE	02/04/04	293.6	16	64	none
h2o.02t	IAEA/IKE	02/04/04	323.6	16	64	none
h2o.03t	IAEA/IKE	02/04/04	373.6	16	64	none
h2o.04t	IAEA/IKE	02/04/04	423.6	16	64	none
h2o.05t	IAEA/IKE	02/04/04	473.6	16	64	none
h2o.06t	IAEA/IKE	02/04/04	523.6	16	64	none
h2o.07t	IAEA/IKE	02/04/04	573.6	16	64	none
h2o.08t	IAEA/IKE	02/04/04	623.6	16	64	none
h2o.09t	IAEA/IKE	02/04/04	647.2	16	64	none
h2o.10t	IAEA/IKE	11/12/04	800	16	64	none
h2o.11t	IAEA/IKE	11/14/04	1000	16	64	none
Deuterium in Heavy Water D_2O (1002)						
d2o.01t	IAEA/IKE	11/09/04	293.6	16	64	none
d2o.02t	IAEA/IKE	11/09/04	323.6	16	64	none
d2o.03t	IAEA/IKE	11/09/04	373.6	16	64	none
d2o.04t	IAEA/IKE	11/09/04	423.6	16	64	none
d2o.05t	IAEA/IKE	11/09/04	473.6	16	64	none
d2o.06t	IAEA/IKE	11/09/04	523.6	16	64	none
d2o.07t	IAEA/IKE	11/09/04	573.6	16	64	none
d2o.08t	IAEA/IKE	11/09/04	643.9	16	64	none
Hydrogen in Zirconium Hydride ZrH (1001)						
h_zrh.01t	IAEA/IKE	11/09/04	293.6	16	64	incoh
h_zrh.02t	IAEA/IKE	11/10/04	400	16	64	incoh
h_zrh.03t	IAEA/IKE	11/10/04	500	16	64	incoh
h_zrh.04t	IAEA/IKE	11/10/04	600	16	64	incoh
h_zrh.05t	IAEA/IKE	11/10/04	700	16	64	incoh
h_zrh.06t	IAEA/IKE	11/10/04	800	16	64	incoh
h_zrh.07t	IAEA/IKE	11/10/04	1000	16	64	incoh
h_zrh.08t	IAEA/IKE	11/10/04	1200	16	64	incoh

The **first column** of the Table contains the ZAID, which is the data set identification to be specified on MCNP(X) MTn cards. The portion of the ZAID before the decimal point provides a shorthand alphanumeric description of the material. The two digits after the decimal point differentiate among different data sets (different temperatures) for the same material. The final character in the ZAID is a "t" which indicates thermal S(α,β) table.
The **second column** of the Table is the evaluated source file. For this MCNP(X) library, all data are from the IAEA/IKE evaluations.
The **thirth column** provides the date that the data table was processed by the NJOY code.
The **fourth column** is the temperature of the data (in degrees Kelvin).
The **fifth column** contains the number of equally-likely discrete secondary cosines provided at each combination of incident and secondary energy for inelastic scattering, and for each incident energy for incoherent elastic scattering.
The **sixth column** gives the number of secondary energies provided for each incident energy for inelastic scattering.
There are three options for the elastic scattering entry in the **seventh column**:

none - no elastic scattering data for this material.
coh -- coherent elastic scattering data provided for this material (Bragg scattering).
incoh - incoherent elastic scattering data provided for this material.

For each moderator an ACE-library was generated named as follows

H_H2O.ace for H in H_2O
D_D2O.iaea for D in D_2O
H_ZrH.iaea for H in ZrH

The associated xsdir file is given below.

xsdir

```
h2o.01t 0.999170 H_H2O.ace 0 1 1 63221 0 0 2.5301E-08
h2o.02t 0.999170 H_H2O.ace 0 1 15819 63221 0 0 2.7886E-08
h2o.03t 0.999170 H_H2O.ace 0 1 31637 63221 0 0 3.2195E-08
h2o.04t 0.999170 H_H2O.ace 0 1 47455 63221 0 0 3.6503E-08
h2o.05t 0.999170 H_H2O.ace 0 1 63273 63221 0 0 4.0812E-08
h2o.06t 0.999170 H_H2O.ace 0 1 79091 63221 0 0 4.5121E-08
h2o.07t 0.999170 H_H2O.ace 0 1 94909 63221 0 0 4.9429E-08
h2o.08t 0.999170 H_H2O.ace 0 1 110727 63221 0 0 5.3738E-08
h2o.09t 0.999170 H_H2O.ace 0 1 126545 63221 0 0 5.5772E-08
h2o.10t 0.999170 H_H2O.ace 0 1 142363 63221 0 0 6.8939E-08
h2o.11t 0.999170 H_H2O.ace 0 1 158181 63221 0 0 8.6174E-08

d2o.01t 1.996800 D_D2O.iaea 0 1 1 63221 0 0 2.5301E-08
d2o.02t 1.996800 D_D2O.iaea 0 1 15819 63221 0 0 2.7886E-08
d2o.03t 1.996800 D_D2O.iaea 0 1 31637 63221 0 0 3.2195E-08
d2o.04t 1.996800 D_D2O.iaea 0 1 47455 63221 0 0 3.6503E-08
d2o.05t 1.996800 D_D2O.iaea 0 1 63273 63221 0 0 4.0812E-08
d2o.06t 1.996800 D_D2O.iaea 0 1 79091 63221 0 0 4.5121E-08
d2o.07t 1.996800 D_D2O.iaea 0 1 94909 63221 0 0 4.9429E-08
d2o.08t 1.996800 D_D2O.iaea 0 1 110727 63221 0 0 5.5487E-08

h_zrh.01t 0.999170 H_ZrH.iaea 0 1 1 91592 0 0 2.5301E-08
h_zrh.02t 0.999170 H_ZrH.iaea 0 1 22911 91592 0 0 3.4470E-08
h_zrh.03t 0.999170 H_ZrH.iaea 0 1 45821 91592 0 0 4.3087E-08
h_zrh.04t 0.999170 H_ZrH.iaea 0 1 68731 91592 0 0 5.1704E-08
h_zrh.05t 0.999170 H_ZrH.iaea 0 1 91641 91592 0 0 6.0322E-08
h_zrh.06t 0.999170 H_ZrH.iaea 0 1 114551 91592 0 0 6.8939E-08
h_zrh.07t 0.999170 H_ZrH.iaea 0 1 137461 91592 0 0 8.6174E-08
h_zrh.08t 0.999170 H_ZrH.iaea 0 1 160371 91592 0 0 1.0341E-07
```

8 Conclusions

New thermal neutron scattering law files in ENDF-6 format for hydrogen bound in water, hydrogen bound in zirconium hydride and deuterium bound in heavy water are available as well as thermal scattering data sets for use in the Monte Carlo codes MCNP and MCNPX. The data are given at a variety of temperatures.

The adequacy of thermal scattering law data was re-considered in view of enhanced computational capabilities and availability of modern computational tools. The following conclusions can be drawn:

- There were hardly any new experimental measurements performed since the time the thermal scattering methods were developed.
- Existing models are able to describe available experimental data reasonably well.
- The generated data for the three moderator materials have been tested quite extensively and in addition compared with the files given in ENDF/B-VI.3 or ENDF/B-VI.8.
- The generating and processing chain for the thermal neutron scattering files with NJOY-99.90 was carefully investigated and necessary updates are given.
- New thermal neutron scattering libraries are available from the IAEA-NDS web site.

9 References

[1] V. McLane, Ed., "ENDF-102: Data Formats and Procedures for the Evaluated Nuclear Data File ENDF-6," Brookhaven National Laboratory report BNL-NCS-44945 –01/04-Rev. (April 2001), http://www.nndc.bnl.gov/nndcscr/documents/endf/endf102/.

[2] J. U. Koppel and D. H. Houston, "Reference Manual for ENDF Thermal Neutron Scattering Data," General Atomics report GA-8774 revised and reissued as ENDF-269 by the National Nuclear Data Center at the Brookhaven National Laboratory (July 1978).

[3] J. U. Koppel, J. R. Triplett, and Y. D. Naliboff, "GASKET: A Unified Code for Thermal Neutron Scattering," General Atomics report GA-7417 (Rev.) (March 1967).

[4] R. E. MacFarlane, "New Thermal Neutron Scattering Files for ENDF/B-VI, Release 2", LA-12639-MS (ENDF-356), (March 994).

[5] R. E. MacFarlane, D. W. Muir, "The NJOY Nuclear Data Processing System", LA-12740-M (1994).

[6] J. Keinert, M. Mattes, "JEF-1 Scattering Law Data", IKE 6-147 / JEF Report 2 / JEF/DOC 41.2 (1984).

[7] L. van Hove, "Correlations in Space and Time and Born Approximation Scattering in Systems of Interacting Particles", Phys. Rev. 95, 249 (1954).

[8] G. H. Vineyard, " Scattering of Slow Neutrons by a Liquid", Phys. Rev. 110, 999 (1958).

[9] K. Sköld, "Small Energy Transfer Scattering of Cold Neutrons from Liquid Argon", Phys.Rev.Lett. 19, 1023 (1967).

[10] A. Eucken, "Zur Kenntnis der Konstitution des Wassers", Nachr. Akad. Wiss., Göttingen, Math. Phys. Kl. 2, 38 (1946).

[11] H. Bertagnolli, Die Struktur des Wassers - eine Mischung von Würfeln und planaren Vierringen", Angew. Chem. 104, 1615 (1992).

[12] D. I. Page, B. C. Haywood, "The HARWELL Scattering Law Programme: Frequency Distributions of Moderators", AERE-R 5778 (1968).

[13] T. Springer, "Die Streuung von langsamen Neutronen an Wasser, Eis und Wasserdampf", Nukleonik 3, 110 (1961).

[14] J. F. Thomson, "Biological Effects of Deuterium; Physical Properties of Deuterium", http://www.cem.msu.edu/~cem181h/projects/98/deuterium/properties.htm

[15] Ph. M. Kanarev, "Energy Balance of Fusion Processes of Molecules of Oxygen, Hydrogen and Water", http://guns.connect.fi/innoplaza/energy/story/Kanarev/water/

[16] C. H.Uffindell**,** A. I. Kolesnikov, J-C. Li, J. Mayers, ”Inelastic neutron scattering study of water in the sub- and supercrital region”, Physica B, 276-278 (2000).

[17] P. Zetterström, A. K. Soper and P. Schofield, “Inelastic neutron scattering of light and heavy water at high incident energies”; Molecular Physics, 90, No.5, 773 (1997).

[18] F. Bischoff et al., “Low Energy Neutron Inelastic Scattering”, RPI-328-87 (1967).

[19] D. E. Parks, M S. Nelkin, J. R. Beyster, and N. F. Wikner, Slow Neutron Scattering and Thermalization, W. A. Benjamin, Inc. (New York, 1970).

[20] J. R. Beyster, “Neutron Scattering from Light Water”, Nucl.Sci.Eng. 31, 254 (1968).

[21] J. L. Russell, J. M. Neill, J. R. Brown, “Total Cross Section Measurements of H_2O”, GA-7581 (1966).

[22] K. Heinloth, ”Scattering of Subthermal Neutrons of H_2O, CH_2O_2 and C_6H_6”, Z. Physik 163, 218 (1961).

[23] K. N. Zaitsev, V. N. Petrov, S. P. Kuznetsov, O. A. Langer, I. V. Meshkov, A. D. Perekrestenko, “The Total Cross Sections of the Interaction of ultracold Neutrons with H_2O and D_2O”, Sov. J. Atomic Energy 70, 238 (1991).

[24] M. Dritsa, A. Kostikas, “Total Cross-Section of Water at Room Temperature and 200C”, EANDC (OR)-63L (1967).

[25] S. B. Herdade, M. J. Bechara, C. Rodriguez, L. A. Vinhas, “Neutron Cross- Sections of Polyethylene and Light Water”, (1973), EXFOR 30229001.

[26] H. D. Lemmel, “Bestimmung der Diffusionskonstanten D(E,T) und Dv(T) thermischer Neutronen in H_2O, Phenylen, $ZrH_{1.92}$ und D_2O durch Messung der Streuwinkelverteilungen $4\pi/\sigma\ d\sigma/d\Omega$.”, Teil I: H_2O, Nukleonik 7, 265 (1965).

[27] C. Reinsch, “Messung des differentiellen Wirkungsquerschnittes und des mittleren logarithmischen Energieverlustes bei der Streuung langsamer Neutronen an Wasser und Eis”, Z. Physik 163, 424 (1961).

[28] K. Inoue, N. Otomo, H. Iwasa, H. Kiyanagi, “Slow Neutron Spectra in Cold Moderators.”, J. Nucl. Sci. Technol. 11, 60 (1974).

[29] J. Keinert, “Neutronenthermalisierung in Metallhydriden”,Thesis. IKE 6-50 (1970).

[30] J. Keinert, “Zur Neutron-Proton-Streuung in Zirkonhydrid”, ATKE 17, 209 (1971).

[31] E. L. Slaggie, "Central Force Lattice Dynamical Model for Zirconium Hydride," General Atomic report GA-8132 (July 1967).

[32] A. C. Evans et al., “Neutron-scattering study of the impulse approximation in ZrH_2”, Phys- Rev. B, 53,3023 (1996).

[33] G. G. Libowitz, “The Solid State Chemistry of Binary Metal Hydrides”, Benjamin Inc. New York (1965).

[34] F. Bischoff et al., “Low Energy Neutron Inelastic Scattering”, RPI-328 (1966).

[35] S. N. Purohit et al., “Inelastic Neutron Scattering in Metal Hydrides, UC and UO2, and Applications of the Scattering Law”, IAEA Symposium on Neutron Thermalisation and Reactor Spectra, Ann Arbor, Vol. I, p.407 (1967).

[36] G. Ehret, “Streuung langsamer Neutronen an Zirkonhydrid”, Thesis, Universität Karlsruhe (1969).

[37] G. W. Carriveau, “Single Differential Cross Section of Zr-Hydride”, GA-8345 (1967).

[38] S. Kornbichler, “Bestimmung der Diffusionskonstanten $D(E_0,T)$ und $\langle Dv(T)\rangle$ thermischer Neutronen in H_2O, Phenylen, $ZrH_{1.92}$ und D_2O durch Messung der Streuwinkelverteilungen. II. Zirkonhydrid und schweres Wasser”, Nukleonik 7, 281 (1965).

[39] W. L. Whittemore, “Differential Neutron Thermalization”, GA-5554 (1964).

[40] U. Schmidt, “Untersuchung der Wasserstoff- und Deuteriumschwingungen in Metallhydriden, -hydrodeuteriden und –deuteriden mittels totaler Neutronen-wirkunsquerschnitte”, ATKE, 12, 385 (1967).

[41] W. L. Whittemore, “Neutron Interaction in Zirconium Hydride”; GA-4490 (1958).

[42] “Experimental and Theoretical Neutron Spectra”; compiled by J. C. Young, and D. Huffmann,GA-5319 (1964).

[43] W. Bernnat, private communication, 2004.

[44] W. Bernnat, D. Emendörfer, J. Keinert, M. Mattes, “Evaluation of Neutron Cross-Sections for Liquid Hydrogen and Deuterium for the Design of Cold”, Neutron Sources”, Proc. Int. Conf. Nuclear Data for Science and Technology, Mito 1988, p. 477.

[45] S. Kornbichler, “Bestimmung der Diffusionskonstanten $D(E_0,T)$ und $\langle Dv(T)\rangle$ thermischer Neutronen in H_2O, Phenylen, $ZrH_{1.92}$ und D_2O durch Messung der Streuwinkelverteilungen. II. Zirkonhydrid und schweres Wasser”, Nukleonik 7, 281 (1965).

[46] T. Springer, “Transmissions- und Streuexperimente mit langsamen Neutronen am FRM-Reaktor”, Nukleonik 6, 87 (1964).

[47] O. K. Harling, “Slow Neutron Inelastic Scattering and the Dynamics of Heavy Water”, NSE, 33, 41 (1968).

[48] F. Kropff, J. R. Latorre, J. R. Granada, C. Castro Madero, “Total Neutron Cross-Section of D_2O at 20 °C between 0.0005 and 10 eV”, EXFOR 30283001 (1984).

[49] S. Dritsa, N. Gaitanis, “Total Neutron Cross Section of D_2O”, EXFOR 20038001 (1983).

[50] U. Schmidt, “Untersuchung der Wasserstorr- und Deuteriumschwingungen in Metallhydriden, -hydrodeuteriden und –deuteriden mittels totaler Neutronen-wirkunsquerschnitte”, ATKE, 12, 385 (1967).

10 APPENDIX

10.1 Updates to NJOY-99.90 for the modules THERMR, LEAPR, ACER

In generating and processing the new thermal neutron scattering data in ENDF-6 and ACE format updates to NJOY-99.90 were necessary for a correct representation of the evaluated data as well as the processed data. Some corrections concern also other moderator materials. The updates listed below are limit to the modules LEAPR, THERMR and ACER.

```
*ident up_thermr
*/ thermr - M. Mattes/IKE ---------------------------------------mm
*/    increase array size for IKE evaluations
*d thermr.101
       dimension a(800000)
*d thermr.131
      namax=800000
*/
*/    fix reading long TAB1 records
*i thermr.1543
      ll=loc
      do while (nb.ne.0)
        ll=ll+nw
        call moreio(nendf,0,0,a(ll),nb,nw)
      enddo
*i thermr.1602
      ll=loc
      do while (nb.ne.0)
        ll=ll+nw
        call moreio(nendf,0,0,a(ll),nb,nw)
      enddo
*/
*/ ------------------------------------------------------------mm
*/ident up2_thermr
*/    maximum.energy transfer at higher temperatures (print only)
*i thermr.1622
      if (lat.eq.1) tmax=tmax*tevz/(bk*temp)
*/ ---------------------------------------------------end up2_thermr
*ident up3_thermr
*/   more incident energies necessary for ZrH for an adequate
*/   represention of the neutron scattering xs in comparison
*/   with experimental results (.1 < E_i < 1 eV)
*d thermr.1422,thermr.1423
       dimension egrid(79)
       dimension ubar(79)
*d thermr.1427
       data ngrid/79/
*d thermr.1433,thermr.1436
     &  .030613d0,.042757d0,.056925d0,.081972d0,
     *      .1d0, .111573d0, .12d0, .13d0, .145728d0, .16d0, .17d0,
     &  .184437d0,
     *    .195d0, .2277d0, .24d0, .2510392d0,.2705304d0,.2907501d0,
     &  .3011332d0,.3206421d0,.3576813d0,
     *   .38d0, .4d0, .4170351d0,  .44d0, .48d0, .5032575d0, .53d0,
     &   .56d0, .59d0,  .6249328d0, .65d0, .69d0, .72d0, .75d0,
     *   .7821141d0, .82d0, .89d0, .9506956d0,1.0137432d0,1.1664337d0,
*d thermr.1455,thermr.1458
     &  .030613e0,.042757e0,.056925e0,.081972e0,
     *      .1e0, .111573e0, .12e0, .13e0, .145728e0, .16e0, .17e0,
```

```
     &  .184437e0,
     *    .195e0, .2277e0, .24e0, .2510392e0,.2705304e0,.2907501e0,
     &  .3011332e0,.3206421e0,.3576813e0,
     *   .38e0, .4e0, .4170351e0,  .44e0, .48e0, .5032575e0, .53e0,
     &   .56e0, .59e0,  .6249328e0, .65e0, .69e0, .72e0, .75e0,
     *   .7821141e0, .82e0, .89e0, .9506956e0,1.0137432e0,1.1664337e0,
*/
*/ ------------------------------------------------end up3_thermr
*ident up1_leapr
*/
*/ if number(>200) for alpha and/or beta values then
*/           increase array sizes plus working buffers
*/    e.g. beta(200) -> beta(400) for H2O
*d leapr.164
       common/ab/nalpha,nbeta,naint,nbint,alpha(200),beta(400)
*d leapr.173
       common/lstore/a(7500000)
*d leapr.178
       data nbmax,namax/400,200/
*d leapr.189
       maxa=7500000
*d leapr.391
       mscr=4000
*d leapr.420
       common/ab/nalph1,nbeta1,naint,nbint,alph1(200),beta1(400)
*d leapr.426
       dimension maxt(400)
*d leapr.794
       common/ab/nalpha,nbeta,naint,nbint,alpha(200),beta1(400)
*d leapr.1252
       common/ab/nalpha1,nbeta1,naint,nbint,alpha(200),beta1(400)
*d leapr.1852
       common/ab/nalph1,nbeta1,naint,nbint,alpha(200),beta1(400)
*/
*/    IKE evaluation of H(H2O) creates more pairs of alpha
*/    and S(alpha,beta) than npage
*i leapr.3122
               l_mm=1+nw
               do while (nb.ne.0)
                    call moreio(0,nout,nprnt,scr(l_mm),nb,nw)
                    l_mm=l_mm+nw
               enddo
*/ ------------------------------------------------end up1_leapr
*ident up2_leapr
*/     for H(H2O), D(D2O) NS should be equal 1
*d leapr.2976,2977
      if(nss.gt.0) scr(5)=6*(nss+1)
      scr(6)=nss
*/ ------------------------------------------------end up2_leapr
*ident up3_leapr
*/  T-eff calculation
*d leapr.1557
       tempf(itemp)=(tbeta+twt)*tempf(itemp)+tsave
*/ ------------------------------------------------end up3_leapr
*ident up4_leapr
*/ generation of more than 10 temperatures
*d leapr.166,167
      common/te/tempr(20),tempf(20),tempf1(20)
      common/dw/dwpix(20),dwp1(20)
*d leapr.179
      data ntmax/20/
*d leapr.600,601
      common/te/tempr(20),tempf(20),tempf1(20)
```

```
      common/dw/dwpix(20),dwp1(20)
*d leapr.797
      common/te/tempr(20),tempf(20),tempf1(20)
*d leapr.1256
      common/te/tempr(20),tempf(20),tempf1(20)
*d leapr.1258
      common/dw/dwpix(20),dwp1(20)
*d leapr.1856
      common/te/tempr(20),tempf(20),tempf1(20)
*d leapr.2651.2652
      common/te/tempr(20),tempf(20),tempf1(20)
      common/dw/dbw(20),dbw1(20)
*/ ---------------------------------------------------end up4_leapr
*ident up5_leapr
*/   correct directory
*i leapr.2797
         scr(5)=scr(5)+1
      if(iel.ne.0) scr(5)=scr(5)+1
*/ ---------------------------------------------------end up5_leapr
*/
*ident up_acer
*/ id-name of thermal data set with 6 characters else blank
*i acer.358
         if (nch.eq.0) nch=6
*/
*/ more than 64 bins  wt(65)
*d acer.13079
      dimension wt(401)
*/
*/ increase of scratch buffer (?)
*d acer.13098
      ninmax=8000
*/
*/ ----------------------------------------------------end---jan05
```

10.2 Inputs to LEAPR

For the three moderator materials light water, heavy water and zirconium hydride the inputs to the module LEAPR of NJOY-90.99 are listed.

10.2.1 H in H_2O

In the following the input to LEAPR for H bound in H_2O is given for the calculation of $S(\alpha,\beta)$ in incoherent approximation for 8 temperatures from 293.6 K up to 647.2 K according to the IKE model.

```
leapr
  40
' H in H2O, IKE model'  /  T=293.6 K +additional Ts  IKE njoy99.90+ dec2003'
 9  1    200/
 1   101  /
  0.99917   20.478    2    /
  1   1   1.585316e+1  3.761  1 /   oxygen as free gas
   182  259  1  /     lat=1
   .0005       .001       .005       .01       .025       .05       .075
   .1          .125       .15        .2        .25        .3        .325
   .35         .375       .4         .425      .45        .475      .5
   .525        .55        .58        .61       .65        .69       .73
   .78         .83        .88        .94       1.        1.08      1.16
  1.24        1.33       1.43       1.54       1.66      1.79      1.94
  2.09        2.26       2.48       2.7127     2.89      3.11      3.38
  3.67        3.98       4.32       4.65       5.0       5.4255    6.
  6.56        7.13       7.6        8.1026     8.8       9.5       10.2
 10.8152     11.7       12.6       13.528     14.4      15.3      16.2051
 17.233      18.2       18.92      20.3       21.63     22.9      24.308
 25.6        27.02      28.4       29.73      31.       32.41     33.44
 34.466      36.15      37.18      38.8       40.513    41.54     42.57
 44.2        46.0       47.0       48.615     49.6      51.2      52.5
 54.41       55.2       56.72      58.4       59.80     61.2      62.51
 63.8        65.23      66.5       67.90      68.93     70.61     71.64
 72.92       75.9       80.        84.        89.       94.       100.
 105.        113.       120.63     126.       132.      140.      147.
 154.        162.       170.       177.       184.      191.      199.
 208.        218.       227.       237.       246.      255.      265.
 275.72      284.       293.58
 302.        311.       320.       329.       338.      347.      356.
 365.        374.       383.       392.       401.      410.      419.
 428.        437.       446.       455.       464.      473.      482.
 491.        500.       509.       518.       527.      536.      545.
 554.        563.       572.       581.       590.      597.      604.
 611.        618.       625.       632.9 /    end of alpha grid
    0.0        0.005      0.01       0.025      0.05      0.075     0.1
     0.15       0.20       0.250      0.30       0.35      0.40      0.45
     0.50       0.55       0.60       0.65       0.70      0.75      0.80
     0.85       0.90       0.95       1.0        1.05      1.10      1.15
     1.20       1.25       1.30       1.35       1.4       1.45      1.5
     1.55       1.6        1.65       1.7        1.75      1.8       1.85
     1.9        1.95       2.0        2.05       2.1       2.15      2.2
     2.25       2.3        2.35       2.4        2.45      2.5       2.55
     2.6        2.65      2.7127      2.77       2.83      2.90      2.96
     3.03       3.11       3.18       3.26       3.34      3.43      3.52
     3.61       3.71       3.81       3.92       4.03      4.14      4.26
     4.39       4.52       4.65       4.80       4.94      5.10      5.26
   5.4255       5.60       5.78       5.97       6.17      6.37      6.59
     6.81       7.04       7.29       7.54       7.81     8.103      8.37
     8.67       8.98       9.30       9.64      10.        10.4     10.8152
    11.16      11.57      12.0       12.46      12.98     13.528    13.94
    14.48      15.03      15.62     16.2051     16.8      17.233    18.2
  18.92        19.4       19.95      20.7      21.63      22.1      22.66
  23.5        24.308      24.8       25.34     26.2       27.02     27.5
```

```
 28.05      28.9      29.73     30.2      30.76     31.5      32.41
 32.9       33.44     34.       34.466    35.3      36.15     36.6
 37.18      37.9      38.8      39.89     40.2      40.513    41.
 41.54      42.       42.57     43.2      44.2      45.28     46.0
 47.0       47.99     48.3      48.615    49.6      50.67     51.2
 51.70      52.5      53.38     53.9      54.41     55.2      56.
 56.72      57.12     58.4      59.80     61.2      62.51     63.8
 65.23      66.5      67.90     68.4      68.93     69.8      70.61
 71.1       71.64     72.2      72.92     73.3340
74.        74.8      75.6      76.4      77.2      78.       78.9
 79.8       80.7      81.6      82.5      83.4      84.3      85.2
 86.1       87.       88.       89.       90.       91.       92.
 93.        94.       95.       96.       97.       98.       99.
100.       101.2     102.4     103.6     104.8     106.      107.2
108.4      109.6     110.8     112.      113.5     115.      116.5
118.       119.5     121.      122.5     124.      125.5     127.
128.5      130.      132.      134.      136.      138.      140.
142.       144.      146.      148.      150.      152.      154.
156.       158.1 /                end of beta grid
  293.6 /                    temperature (K)
0.002542    68 /             frequency distribution
 0.0
 0.010417  0.041671  0.093749  0.166682  0.260457  0.374972  0.510341
 0.666586  0.843707  1.041692  1.260385  1.499907  1.760466  2.041717
 2.343789  2.666650  3.010451  3.338729  3.721638  4.104406  4.542219
 4.980193  5.473275  5.911964  6.240707  6.459711  6.569646  6.569798
 6.350101  5.910588  5.581434  5.197376  4.868524  4.539521  4.265442
 3.991243  3.717142  3.498139  3.278887  3.114840  2.950674  2.846502
 2.747844  2.654690  2.567061  2.484945  2.408355  2.337267  2.271694
 2.211646  2.157112  2.127321  2.115426  2.103531  2.091647  2.079752
 2.067857  2.055962  2.044078  2.032184  2.020289  2.008394  1.996510
 1.984615  1.972720  0.986360  0.000000 /
 0.021739  0.  .4891305 /  weights
 2 /                        discrete oscillators
.205  .436 /                oscillator energies (eV)
 .1630435   .326087  /     oscillator weigths
  323.6 /
0.002542    68 /
 0.0
 0.010274  0.041098  0.092461  0.164391  0.256874  0.369821  0.503327
 0.657423  0.832105  1.027361  1.243055  1.479286  1.736244  2.013628
 2.311551  2.629996  2.969060  3.296833  3.677702  4.063789  4.496955
 4.929182  5.402663  5.820385  6.136398  6.350894  6.450654  6.447689
 6.247174  5.848280  5.538408  5.178377  4.864600  4.551672  4.290382
 4.029290  3.768586  3.556458  3.344402  3.181163  3.012451  2.907611
 2.802694  2.703053  2.607208  2.518125  2.433465  2.356584  2.283830
 2.218029  2.155013  2.114911  2.092962  2.070193  2.048001  2.026644
 2.010179  1.992757  1.975799  1.959260  1.943201  1.929021  1.913881
 1.899183  1.884927  0.939784  0.000000 /
 0.025641  0. 0.4871795   /
 2 /
.205  .436  /
 0.162393167   0.324786333     /
  373.6 /
0.002542    68 /
 0.0
 0.010034  0.040141  0.090311  0.160568  0.250895  0.361226  0.491622
 0.642134  0.812745  1.003447  1.214136  1.444875  1.695825  1.966757
 2.257755  2.568830  2.899988  3.226761  3.604098  3.995381  4.420742
 4.843365  5.284645  5.667974  5.963068  6.170103  6.253226  6.245183
 6.076035  5.743552  5.465272  5.144590  4.855550  4.568990  4.328684
 4.089093  3.850360  3.649553  3.449340  3.287507  3.111478  3.005608
 2.890546  2.780391  2.671210  2.570820  2.473057  2.386776  2.302360
 2.227221  2.150418  2.093534  2.055214  2.014735  1.975758  1.938994
 1.915090  1.888672  1.863453  1.839356  1.816520  1.798624  1.778184
 1.758928  1.740832  0.863370  0.000000 /
 0.032258  0.  0.483871  /
 2 /
.205  .436  /
0.161290333    0.322580667 /
```

```
  423.6 /
0.002542    68 /
 0.0
 0.009837  0.039352  0.088538  0.157413  0.245961  0.354135  0.481965
 0.629520  0.796770  0.983714  1.190275  1.416484  1.662472  1.928080
 2.213364  2.518363  2.842997  3.169966  3.545208  3.942965  4.362235
 4.777004  5.188450  5.539596  5.815341  6.015837  6.083027  6.070001
 5.930849  5.661969  5.413514  5.130075  4.864132  4.602272  4.381576
 4.162104  3.943952  3.753470  3.564092  3.403051  3.219253  3.111997
 2.986626  2.865816  2.743233  2.631452  2.520554  2.424792  2.328696
 2.244177  2.153646  2.080185  2.025755  1.967852  1.912358  1.860430
 1.829182  1.793892  1.760523  1.728966  1.699435  1.677850  1.652167
 1.628393  1.606486  0.791912  0.000000 /
 0.037037   0.    0.4814815    /
 2 /
.205  .436 /
 0.160493833   0.320987667  /
  473.6 /
0.002542    68 /
 0.0
 0.009680  0.038723  0.087126  0.154902  0.242033  0.348491  0.474277
 0.619478  0.784051  0.968000  1.171277  1.393880  1.635911  1.897281
 2.178018  2.478188  2.797623  3.126010  3.500601  3.906212  4.321066
 4.729669  5.113325  5.434147  5.691901  5.886721  5.938498  5.920525
 5.810343  5.602984  5.382920  5.135033  4.890802  4.652241  4.449999
 4.249483  4.050748  3.869703  3.690269  3.529402  3.337276  3.228256
 3.092280  2.960542  2.824323  2.700924  2.576697  2.471255  2.363315
 2.269258  2.164891  2.074858  2.004385  1.929135  1.857196  1.790165
 1.751580  1.707434  1.665929  1.626918  1.590696  1.565402  1.534468
 1.506164  1.480427  0.724627  0.000000 /
 0.040000  0.      0.48    /
 2 /
.205  .436
 .16  .32  /
  523.6 /
0.002542    68 /
 0.0
 0.009513  0.038056  0.085629  0.152238  0.237867  0.342505  0.466124
 0.608828  0.770564  0.951337  1.151131  1.369910  1.607747  1.864622
 2.140537  2.435582  2.749506  3.078892  3.452387  3.865250  4.275248
 4.677276  5.033074  5.323616  5.563322  5.752311  5.788833  5.766004
 5.684512  5.538051  5.346240  5.133698  4.911166  4.695864  4.512058
 4.330471  4.151116  3.979593  3.810179  3.649679  3.449577  3.338950
 3.192683  3.050333  2.900837  2.766136  2.628919  2.514064  2.394579
 2.291232  2.173354  2.067093  1.980891  1.888632  1.800568  1.718731
 1.672960  1.620139  1.570662  1.524351  1.481577  1.452658  1.416584
 1.383849  1.354369  0.657422  0.000000 /
 0.043478  0.      0.478261  /
 2 /
.205  .436
 0.159420333   0.318840667  /
  573.6 /
0.002542    68 /
 0.0
 0.009379  0.037520  0.084423  0.150094  0.234513  0.337687  0.459561
 0.600255  0.759704  0.937919  1.134910  1.350611  1.585066  1.838323
 2.110355  2.401281  2.710765  3.042192  3.415798  3.837144  4.243656
 4.640476  4.969893  5.231451  5.454096  5.637929  5.659497  5.631798
 5.578387  5.491613  5.327099  5.148794  4.946985  4.753968  4.587786
 4.424318  4.263535  4.100869  3.940811  3.780160  3.571540  3.458972
 3.302073  3.148784  2.985695  2.839397  2.688911  2.564388  2.433118
 2.320265  2.188663  2.066032  1.964017  1.854661  1.750387  1.653661
 1.600646  1.539086  1.481577  1.427907  1.378522  1.345931  1.304665
 1.267448  1.234175  0.593138  0.000000 /
 0.045454  0.   0.477273  /
 2 /
.205  .436  /
0.159091        0.318182  /
  623.6 /
0.002542    68 /
```

```
  0.0
  0.009241  0.036971  0.083191  0.147901  0.231083  0.332760  0.452849
  0.591487  0.748599  0.924198  1.118324  1.330876  1.561874  1.811430
  2.079492  2.366205  2.671149  3.004446  3.377992  3.807549  4.210421
  4.601901  4.905032  5.137760  5.343403  5.522043  5.528789  5.496279
  5.470710  5.443103  5.305704  5.161395  4.980206  4.809356  4.660707
  4.515263  4.372950  4.219132  4.068416  3.907689  3.690725  3.576285
  3.408925  3.244872  3.068391  2.910673  2.747111  2.613069  2.470184
  2.347965  2.202827  2.064036  1.946403  1.820161  1.699877  1.588447
  1.528279  1.458090  1.392651  1.331715  1.275806  1.239591  1.193201
  1.151560  1.114547  0.529185  0.000000 /
  0.047620  0.     0.47619 /
  2 /
 .205  .436 /
 0.15873        0.31746   /
   647.2 /
 0.002542    68 /
  0.0
   .009213   .036856   .082933   .147444   .230368   .331730   .451447
   .589657   .746283   .921338  1.114863  1.326758  1.557041  1.805824
  2.073057  2.358883  2.662883  2.995149  3.367539  3.795767  4.197392
  4.587660  4.889854  5.121861  5.326868  5.504956  5.511680  5.479271
  5.453781  5.426260  5.289285  5.145423  4.964795  4.794473  4.646285
  4.501290  4.359418  4.206076  4.055827  3.895597  3.679304  3.565219
  3.398377  3.234830  3.058896  2.901666  2.738610  2.604983  2.462540
  2.340699  2.196011  2.057649  1.940380  1.814529  1.694617  1.583531
  1.523550  1.453578  1.388341  1.327594  1.271858  1.235755  1.189508
  1.147997  1.111098   .527548   .000000 /
  0.049020  0.   0.47549 /
  2 /
 .205  .436 /
 0.158496667    0.316993333   /
' H(H2O)    IKE        EVAL-jan04 Keinert,Mattes                    '
' IKE 6-201             DIST-feb04                       040202     '
'----IKE/IAEA           MATERIAL    1                                '
'-----THERMAL NEUTRON SCATTERING DATA                                '
'------ENDF-6 FORMAT                                                '
'*                                                                 *'
'*-------------------------------------------------------------------*'
'* Temperatures (K)                                                 *'
'*         293.6  323.6  373.6  423.6  473.6  523.6  573.6  647.2 *'
'*                                                                  *'
'* Modifications of the IKE model compared to the JEF-2.2 thermal *'
'* data file:                                                       *'
'*  -   alpha,beta-grid strictly correlated to the phonon spectra *'
'*  -   modification of hindered rotational mode spectrum at high *'
'*      frequencies                                                 *'
'*  -   oscillator frequency omega1=omega3 changed to 0.436 eV    *'
'*  -   optical modes equally weighted                            *'
'*                                                                  *'
'* generated with LEAPR/NJOY-99.90++                IKE jan2004  *'
'*-------------------------------------------------------------------*'
/  end leapr
stop
```

10.2.2 H in ZrH

In the following the input for LEAPR for H bound in ZrH is tabulated for the calculation of S(α,β) in incoherent approximation for 8 temperatures from 293.6 K up to 1200 K according to the IKE physics model.

```
leapr
40
'H in ZrH     IKE model'/
 8  1  200/             8 temperatures
7 107./
.99917 20.478 1 -1/
1  1  90.436  6.37 1/  Zr as free gas /
 147  185 1 /   ---- alpha grid
   .0001      .0003
   .0006       .001      .005      .01       .025      .05       .075
   .1          .125      .15       .2        .25       .3        .325
   .35         .375      .4        .425      .45       .475      .5
   .525        .55       .58       .61       .65       .69       .73
   .7905       .83       .88       .94       1.       1.08      1.16
  1.24        1.33      1.45      1.581      1.7       1.8       1.95
  2.1         2.26      2.3715    2.5        2.65      2.83
  2.96     3.162     3.38
  3.67        3.9525    4.32      4.52       4.743     5.1       5.415
  5.97        6.324
  6.59        7.114     7.54      7.905      8.695     9.486     10.276
 10.830      11.857    12.648    13.438     14.229    15.019     15.810
 16.245      17.2
 18.245      19.4    20.3      21.659    22.9        24.8
 26.2        27.074    28.9     30.2        31.5      32.489    34.
 36.6                  37.904    39.        41.1      43.319
 44.4        45.5      47.7      48.734     50.       51.2      52.5
 53.9        55.149    56.3      58.4       59.564    61.2
 63.8        64.978    66.5      68.4       69.4      70.393    71.6
 73.334      75.808    80.       84.        89.       94.       100.
 105.        113.      120.63    126.       132.      140.      147.
 154.        162.      170.      177.       184.      191.      199.
 208.        218.      227.      237.       246.      255.      265.
 275.72      284.      293.58 / --- beta grid
     0.0       0.005     0.01      0.025     0.05      0.075     0.1
     0.15      0.20      0.250     0.30      0.35      0.40      0.45
     0.50      0.55      0.60      0.65      0.70      0.75    0.7905
     0.85      0.90      0.95      1.0       1.05      1.10      1.15
     1.20      1.25      1.30      1.35      1.4       1.45      1.5
     1.55
     1.581     1.6       1.65      1.7       1.75      1.8       1.85
     1.9       1.95      2.0       2.05      2.1       2.15      2.2
     2.25      2.3       2.35      2.3715
     2.4       2.45      2.5       2.55
     2.6       2.65                2.77      2.83      2.90      2.96
     3.03      3.11      3.162
     3.20      3.26      3.34      3.43      3.52
     3.61      3.71      3.81      3.89      3.9525
     4.03      4.14      4.26
     4.39      4.52      4.65      4.743
     4.84      4.94      5.10      5.26      5.415
     5.533     5.60      5.78      5.97      6.17      6.324
     6.48      6.59
     6.81      6.96      7.114
     7.29      7.54      7.72      7.905     8.15      8.37
     8.695     8.98      9.30      9.486
     9.64     10.       10.276    10.6      10.830    10.95
    11.067
    11.31     11.57     11.857
    12.15     12.46     12.648
    12.98     13.438    13.94     14.229
    14.48     15.019     15.42    15.810     16.       16.245
    16.6      17.4      18.2
    18.8      19.4      20.       20.7      21.659    22.6
  23.5                  24.8                26.2      27.074   27.9
            28.9                  30.2                31.5    32.489
  33.2                  34.                 35.3                36.6
```

```
            37.904    39.                 40.2                41.1
            42.2                43.319    44.4                45.5
  46.6      47.7      48.734    50.                           51.2
            52.5                53.9                55.149    56.3
            57.3      58.4      59.564    61.2                63.8
  64.978    66.5                68.4                69.4    70.393
  71.1                72.2                73.3340 /
293.6/
0.001  181 /     frequency distribution
 0.0
 1.540E-03 6.170E-03 1.387E-02 2.467E-02 3.854E-02 5.550E-02
 7.554E-02 9.866E-02 1.249E-01 1.542E-01 1.865E-01 2.220E-01
 2.605E-01 3.022E-01 3.469E-01 3.947E-01 4.455E-01 4.995E-01
 5.565E-01 6.166E-01 0.000E+00 0.000E+00 0.000E+00 0.000E+00
 0.000E+00 0.000E+00 0.000E+00 0.000E+00 0.000E+00 0.000E+00
 0.000E+00 0.000E+00 0.000E+00 0.000E+00 0.000E+00 0.000E+00
 0.000E+00 0.000E+00 0.000E+00 0.000E+00 0.000E+00 0.000E+00
 0.000E+00 0.000E+00 0.000E+00 0.000E+00 0.000E+00 0.000E+00
 0.000E+00 0.000E+00 0.000E+00 0.000E+00 0.000E+00 0.000E+00
 0.000E+00 0.000E+00 5.882E-07 1.765E-06 2.941E-06 4.118E-06
 5.294E-06 6.471E-06 7.647E-06 8.824E-06 1.000E-05 4.176E-05
 7.353E-05 1.053E-04 1.371E-04 1.688E-04 2.006E-04 2.324E-04
 2.641E-04 6.665E-04 1.439E-03 2.212E-03 2.985E-03 3.758E-03
 4.531E-03 5.304E-03 6.077E-03 6.850E-03 1.793E-02 2.900E-02
 4.008E-02 5.115E-02 6.223E-02 7.330E-02 8.438E-02 9.545E-02
 1.476E-01 2.407E-01 3.339E-01 4.270E-01 5.202E-01 6.133E-01
 7.065E-01 7.996E-01 8.928E-01 1.116E+00 1.384E+00 1.705E+00
 2.086E+00 2.534E+00 3.057E+00 3.661E+00 4.353E+00 5.140E+00
 6.027E+00 7.017E+00 8.112E+00 9.311E+00 1.061E+01 1.201E+01
 1.350E+01 1.506E+01 1.669E+01 1.836E+01 2.006E+01 2.176E+01
 2.344E+01 2.507E+01 2.662E+01 2.807E+01 2.939E+01 3.055E+01
 3.154E+01 3.233E+01 3.291E+01 3.326E+01 3.338E+01 3.326E+01
 3.291E+01 3.233E+01 3.154E+01 3.055E+01 2.939E+01 2.807E+01
 2.662E+01 2.506E+01 2.344E+01 2.176E+01 2.006E+01 1.836E+01
 1.669E+01 1.506E+01 1.350E+01 1.201E+01 1.061E+01 9.311E+00
 8.112E+00 7.017E+00 6.027E+00 5.140E+00 4.353E+00 3.661E+00
 3.057E+00 2.534E+00 2.086E+00 1.705E+00 1.384E+00 1.116E+00
 8.928E-01 7.263E-01 5.598E-01 4.505E-01 3.412E-01 2.717E-01
 2.021E-01 1.593E-01 1.164E-01 9.082E-02 6.519E-02 0. /
0. 0. 1. 0./
0/
-400./
-500./
-600./
-700./
-800./
-1000./
-1200./
' H(ZrH)    IKE        EVAL-      Keinert,Mattes                    '
' IKE 6-201 (2004)     DIST-feb04                       040202     '
'----INDL-IKE          MATERIAL    7                                 '
'-----THERMAL NEUTRON SCATTERING DATA                                '
'------ENDF-6 FORMAT                                                '
'*                                                                  *'
'*------------------------------------------------------------------*'
' TEMPERATURES = 293.6 400 500 600 700 800 1000 1200 DEG K.'/
'*                                                                  *'
'*    Zr is treated as free gas                                     *'
'*------------------------------------------------------------------*'
'*  LEAPR/NJOY-99.90+        generated at IKE Stuttgart feb.2004  *'
/  end leapr                   -------------------------------------
stop
```

10.2.3 D in D_2O, incoherent part only.

In the following the input to LEAPR for D bound in D_2O is tabulated for the calculation of $S(\alpha,\beta)$ in incoherent approximation for 293.6 K. D-D interference scattering is **not** included as this is not treated in LEAPR.

```
leapr
  40
' D in D2O  T=293.6 K only incoherent part  IKE njoy99.90+ feb2004'
 1  1    /
 1   111  /
  1.9968    3.395    2    /
  1   1   1.585316e+1  3.761  1 /
   159  277  1  /                lat=1
    0.0001    0.0002    0.0004    0.0006    0.0008    0.0010    0.0015
    0.0020    0.0025    0.0030    0.0040    0.0050    0.0060    0.0080
    0.0100    0.0150    0.0200    0.0250    0.0350    0.0500    0.0600
    0.0750    0.0850    0.1000    0.1250    0.1500    0.1750    0.2000
    0.2250    0.2500    0.2750    0.3000    0.3250    0.3500    0.3750
    0.4000    0.4250    0.4500    0.4750    0.5000    0.5300    0.5600
    0.5900    0.6200    0.6600    0.7000    0.7500    0.8000    0.8500
    0.9000    0.9600    1.0200    1.1000    1.2000    1.2800    1.3500
    1.4250    1.5000    1.5700    1.6500    1.7500    1.8500    1.9500
    2.0500    2.2000    2.3500    2.5500    2.7500    3.0300    3.2600
    3.5300    3.8600    4.1900    4.5000    4.9500    5.3400    5.7800
    6.1800    6.5200    6.9000    7.4000    7.9500    8.2500    8.7000
    9.6000   10.4000   11.4000   12.4400   13.5000   14.7000   16.0000
   17.2000   18.7000   20.0000   21.1000   22.5000   23.4000   24.5000
   25.5000   27.0000   29.2000   31.7000   33.2000   34.6000   36.0000
   37.2000   39.1000   41.0000   42.5000   44.2000   46.0000   48.5000
   50.6000   53.4000   54.1000   55.2000   57.6000   60.0000   62.2000
   63.9000   65.7000   67.1000   68.5000   69.7000   71.0000   72.0000
   73.3000   74.7000   76.4000   78.0000   79.5000   81.4000   83.2000
   84.9000   86.7000   88.5000   90.5000   92.5000   94.5000   96.6000
   98.7000  100.9000  103.0000  105.2000  108.0000  112.4000  114.7000
  117.0000  119.4000  122.2000  125.0000  128.0000  132.0000  136.2000
  138.0000  140.0000  142.0000  144.0000  146.9000 / end of alpha grid
    0.0000    0.0025    0.0050    0.0075    0.0100    0.0150    0.0200
    0.0250    0.0300    0.0350    0.0500    0.0600    0.0750    0.0850
    0.1000    0.1250    0.1500    0.1750    0.2000    0.2250    0.2500
    0.2750    0.3000    0.3250    0.3500    0.3750    0.4000    0.4250
    0.4500    0.4750    0.5000    0.5250    0.5500    0.5750    0.6000
    0.6250    0.6500    0.6750    0.7000    0.7250    0.7500    0.7750
    0.7984    0.8250    0.8500    0.8750    0.9000    0.9250    0.9500
    0.9750    1.0000    1.0200    1.0500    1.0750    1.1000    1.1250
    1.1500    1.1750    1.2000    1.2250    1.2500    1.2750    1.3000
    1.3500    1.4000    1.4500    1.5000    1.5500    1.5968    1.6500
    1.7000    1.7500    1.8000    1.8500    1.9104    1.9500    2.0000
    2.0500    2.1000    2.1500    2.2000    2.2500    2.3000    2.3500
    2.3952    2.4500    2.5000    2.5500    2.5911    2.6500    2.7000
    2.7500    2.8000    2.8400    2.8800    2.9300    2.9800    3.0300
    3.0800    3.1400    3.1936    3.2600    3.3500    3.4400    3.5300
    3.6200    3.7100    3.8208    3.8600    3.9200    3.9920    4.0300
    4.0800    4.1400    4.1900    4.2500    4.3100    4.3700    4.4300
    4.5000    4.5700    4.6500    4.7200    4.7904    4.8700    4.9500
    5.0200    5.1000    5.1822    5.2500    5.3400    5.5000    5.5888
    5.6262    5.6600    5.7311    5.7800    5.8800    5.9700    6.0700
    6.1700    6.2800    6.3872    6.5200    6.6500    6.7700    6.9000
    7.0200    7.1856    7.4000    7.6416    7.7733    7.9840    8.1000
    8.2500    8.4500    8.7000    9.0000    9.3000    9.5520    9.9500
   10.3644   10.8000   11.0000   11.2000   11.4622   11.6500   12.1000
   12.6000   13.1000   13.3593   13.6000   13.8000   14.0000   14.2000
   14.5500   15.1000   15.2832   15.5466   15.7000   16.0000   16.1700
   16.3500   16.5000   16.7000   16.9000   17.1933   17.5000   18.1377
   18.7000   18.9000   19.1040   19.3000   19.5000   19.7500   20.0000
   20.3500   20.7288   21.1000   21.8000   22.2000   22.5500   22.9244
   23.4000   23.9000   24.3000   24.5000   24.8000   25.1000   25.3000
   25.5000   26.0000   26.4000   26.7186   27.0000   27.6000   28.2000
   28.6555   29.7000   30.3000   31.0000   31.7000   32.4000   33.2000
   34.3866   34.8000   35.2000   36.0000   36.6000   37.2000   37.9000
   38.5000   39.1000   39.8000   40.0900   40.5000   41.0000   41.5000
   42.0000   42.5000   43.0000   43.6000   44.2000   44.8000   45.4000
   45.8500   46.0000   46.7000   47.5000   48.5000   49.5000   50.6000
```

```
  51.5800   52.5000   53.4400   54.1000   55.2000   56.5000   57.6000
  58.7000   60.0000   61.1000   62.2000   63.5000   64.6000   65.7000
  67.0000   67.5000   68.0000   68.5000   70.5000   71.0000   71.5000
  72.0000   72.5000   72.9000   73.3340 / end of beta grid
  293.6 /
0.00028879   572 /
 0.0
2.23783E-03 6.65181E-03 1.45127E-02 2.68802E-02 4.31287E-02 5.93772E-02
7.56256E-02 9.94981E-02 1.26215E-01 1.52931E-01 1.86715E-01 2.24982E-01
2.63249E-01 3.01516E-01 3.41114E-01 3.91436E-01 4.41758E-01 4.92080E-01
5.49531E-01 6.10859E-01 6.72188E-01 7.33517E-01 8.08931E-01 8.87053E-01
9.65175E-01 1.04330E+00 1.12142E+00 1.19954E+00 1.27766E+00 1.36823E+00
1.46831E+00 1.56839E+00 1.66847E+00 1.76854E+00 1.86862E+00 1.96870E+00
2.07546E+00 2.19817E+00 2.32088E+00 2.44360E+00 2.56631E+00 2.68902E+00
2.81173E+00 2.93444E+00 3.06836E+00 3.20761E+00 3.34687E+00 3.48852E+00
3.63893E+00 3.78934E+00 3.93975E+00 4.09489E+00 4.25695E+00 4.41901E+00
4.58107E+00 4.74958E+00 4.92244E+00 5.09530E+00 5.26966E+00 5.45372E+00
5.63779E+00 5.82185E+00 6.00950E+00 6.20457E+00 6.39964E+00 6.59471E+00
6.79904E+00 7.00486E+00 7.21067E+00 2.11225E+00 2.17407E+00 2.23589E+00
2.29772E+00 2.36082E+00 2.42789E+00 2.49496E+00 2.56204E+00 2.62911E+00
2.69618E+00 2.76325E+00 2.83032E+00 2.90194E+00 2.97370E+00 3.04545E+00
3.11720E+00 3.18895E+00 3.26071E+00 3.33246E+00 3.40460E+00 3.47690E+00
3.54921E+00 3.62151E+00 3.69381E+00 3.76612E+00 3.83842E+00 3.91072E+00
3.98288E+00 4.05505E+00 4.12721E+00 4.19938E+00 4.27155E+00 4.34371E+00
4.41588E+00 4.48816E+00 4.56046E+00 4.63277E+00 4.70507E+00 4.77737E+00
4.84968E+00 4.92198E+00 4.98916E+00 5.05196E+00 5.11476E+00 5.17756E+00
5.24036E+00 5.30316E+00 5.36596E+00 5.42543E+00 5.47578E+00 5.52612E+00
5.57647E+00 5.62682E+00 5.67717E+00 5.72752E+00 5.77787E+00 5.82674E+00
5.87480E+00 5.92287E+00 5.97093E+00 6.01899E+00 6.06706E+00 6.11512E+00
6.16434E+00 6.21543E+00 6.26652E+00 6.31762E+00 6.36871E+00 6.41981E+00
6.47090E+00 6.52065E+00 6.55917E+00 6.59769E+00 6.63621E+00 6.67472E+00
6.71324E+00 6.75176E+00 6.79028E+00 6.82714E+00 6.86226E+00 6.89738E+00
6.93250E+00 6.96762E+00 7.00274E+00 7.03786E+00 7.07276E+00 7.10689E+00
7.14101E+00 7.17514E+00 7.19185E+00 7.20289E+00 7.21394E+00 7.22498E+00
7.23254E+00 7.23990E+00 7.24726E+00 7.25334E+00 7.25132E+00 7.24930E+00
7.24727E+00 7.23793E+00 7.22505E+00 7.21216E+00 7.19928E+00 7.18822E+00
7.17744E+00 7.16666E+00 7.15412E+00 7.11190E+00 7.06968E+00 7.02745E+00
6.98064E+00 6.93069E+00 6.88073E+00 6.83077E+00 6.77766E+00 6.72367E+00
6.66968E+00 6.61569E+00 6.56171E+00 6.50772E+00 6.45373E+00 6.39848E+00
6.34201E+00 6.28554E+00 6.22908E+00 6.17261E+00 6.11615E+00 6.05968E+00
5.99975E+00 5.92889E+00 5.85804E+00 5.78718E+00 5.71632E+00 5.64546E+00
5.57460E+00 5.50375E+00 5.43808E+00 5.37555E+00 5.31303E+00 5.25050E+00
5.18798E+00 5.12546E+00 5.06293E+00 5.00011E+00 4.93676E+00 4.87341E+00
4.81006E+00 4.74670E+00 4.68335E+00 4.62000E+00 4.55785E+00 4.50960E+00
4.46135E+00 4.41311E+00 4.36486E+00 4.31661E+00 4.26837E+00 4.22012E+00
4.17259E+00 4.12591E+00 4.07922E+00 4.03253E+00 3.98585E+00 3.93916E+00
3.89247E+00 3.84715E+00 3.80762E+00 3.76809E+00 3.72856E+00 3.68904E+00
3.64951E+00 3.60998E+00 3.57046E+00 3.53257E+00 3.49484E+00 3.45710E+00
3.41937E+00 3.38163E+00 3.34390E+00 3.30616E+00 3.27013E+00 3.23503E+00
3.19993E+00 3.16483E+00 3.12973E+00 3.09463E+00 3.05953E+00 3.02453E+00
2.99285E+00 2.96117E+00 2.92950E+00 2.89782E+00 2.86615E+00 2.83447E+00
2.80279E+00 2.77404E+00 2.74622E+00 2.71840E+00 2.69058E+00 2.66276E+00
2.63494E+00 2.60712E+00 2.58266E+00 2.56176E+00 2.54085E+00 2.51995E+00
2.49905E+00 2.47814E+00 2.45724E+00 2.43634E+00 2.41290E+00 2.38907E+00
2.36525E+00 2.34142E+00 2.31760E+00 2.29377E+00 2.26995E+00 2.24957E+00
2.23152E+00 2.21348E+00 2.19544E+00 2.17740E+00 2.15936E+00 2.14132E+00
2.12363E+00 2.10669E+00 2.08976E+00 2.07282E+00 2.05588E+00 2.03894E+00
2.02200E+00 2.00510E+00 1.98906E+00 1.97303E+00 1.95699E+00 1.94095E+00
1.92491E+00 1.90887E+00 1.89283E+00 1.87760E+00 1.86342E+00 1.84923E+00
1.83505E+00 1.82086E+00 1.80667E+00 1.79249E+00 1.77882E+00 1.76780E+00
1.75678E+00 1.74576E+00 1.73475E+00 1.72373E+00 1.71271E+00 1.70169E+00
1.69227E+00 1.68304E+00 1.67381E+00 1.66459E+00 1.65536E+00 1.64613E+00
1.63690E+00 1.62623E+00 1.61466E+00 1.60309E+00 1.59152E+00 1.57995E+00
1.56838E+00 1.55681E+00 1.54525E+00 1.53368E+00 1.52211E+00 1.51054E+00
1.50101E+00 1.49324E+00 1.48547E+00 1.47770E+00 1.46993E+00 1.46215E+00
1.45438E+00 1.44661E+00 1.43884E+00 1.43107E+00 1.42329E+00 1.41563E+00
1.40810E+00 1.40056E+00 1.39303E+00 1.38550E+00 1.37796E+00 1.37043E+00
1.36290E+00 1.35536E+00 1.34783E+00 1.34030E+00 1.33276E+00 1.32523E+00
1.31770E+00 1.31016E+00 1.30372E+00 1.29810E+00 1.29248E+00 1.28685E+00
1.28123E+00 1.27561E+00 1.26999E+00 1.26437E+00 1.25875E+00 1.25313E+00
1.24751E+00 1.24189E+00 1.23627E+00 1.23065E+00 1.22503E+00 1.21941E+00
1.21379E+00 1.20817E+00 1.20286E+00 1.19872E+00 1.19457E+00 1.19042E+00
1.18628E+00 1.18213E+00 1.17798E+00 1.17383E+00 1.16969E+00 1.16554E+00
1.16139E+00 1.15725E+00 1.15310E+00 1.14895E+00 1.14480E+00 1.14066E+00
1.13651E+00 1.13236E+00 1.12822E+00 1.12525E+00 1.12246E+00 1.11968E+00
1.11690E+00 1.11412E+00 1.11133E+00 1.10855E+00 1.10577E+00 1.10298E+00
1.10020E+00 1.09742E+00 1.09464E+00 1.09185E+00 1.08907E+00 1.08629E+00
1.08351E+00 1.08072E+00 1.07794E+00 1.07532E+00 1.07286E+00 1.07039E+00
```

```
 1.06793E+00 1.06547E+00 1.06300E+00 1.06054E+00 1.05807E+00 1.05561E+00
 1.05315E+00 1.05068E+00 1.04822E+00 1.04575E+00 1.04329E+00 1.04083E+00
 1.03836E+00 1.03590E+00 1.03344E+00 1.03097E+00 1.02872E+00 1.02651E+00
 1.02431E+00 1.02210E+00 1.01990E+00 1.01770E+00 1.01549E+00 1.01329E+00
 1.01108E+00 1.00888E+00 1.00667E+00 1.00447E+00 1.00226E+00 1.00006E+00
 9.97854E-01 9.95649E-01 9.93444E-01 9.91240E-01 9.89196E-01 9.87341E-01
 9.85485E-01 9.83630E-01 9.81775E-01 9.79919E-01 9.78064E-01 9.76209E-01
 9.74353E-01 9.72498E-01 9.70643E-01 9.68787E-01 9.66932E-01 9.65076E-01
 9.63221E-01 9.61366E-01 9.59510E-01 9.57655E-01 9.55840E-01 9.54361E-01
 9.52883E-01 9.51404E-01 9.49925E-01 9.48446E-01 9.46967E-01 9.45489E-01
 9.44010E-01 9.42531E-01 9.41052E-01 9.39573E-01 9.38094E-01 9.36616E-01
 9.35137E-01 9.33658E-01 9.32179E-01 9.30700E-01 9.29221E-01 9.28345E-01
 9.27662E-01 9.26980E-01 9.26298E-01 9.25616E-01 9.24933E-01 9.24251E-01
 9.23569E-01 9.22887E-01 9.22205E-01 9.21522E-01 9.20840E-01 9.20158E-01
 9.19476E-01 9.18794E-01 9.18112E-01 9.17429E-01 9.16747E-01 9.16123E-01
 9.15585E-01 9.15047E-01 9.14508E-01 9.13970E-01 9.13432E-01 9.12894E-01
 9.12356E-01 9.11920E-01 9.11513E-01 9.11106E-01 9.10593E-01 9.09858E-01
 9.09123E-01 9.08387E-01 9.07599E-01 9.06759E-01 9.05920E-01 9.05081E-01
 9.04241E-01 9.03402E-01 9.02563E-01 9.01723E-01 9.00884E-01 9.00045E-01
 8.99205E-01 8.98242E-01 8.97243E-01 8.96244E-01 8.95245E-01 8.94246E-01
 8.93247E-01 8.92248E-01 8.91254E-01 8.90290E-01 8.89326E-01 8.88362E-01
 8.87398E-01 8.86434E-01 8.85470E-01 8.84506E-01 8.32777E-01 7.74746E-01
 7.16718E-01 6.58685E-01 6.00634E-01 5.42581E-01 4.84530E-01 4.24898E-01
 3.61039E-01 2.97177E-01 2.33318E-01 1.74155E-01 1.16104E-01 5.80507E-02
 0.00000E+00 /
  0.05  0.  .45 /
  2 /
 .145  .338
  .16666667   .33333333    /
' D(D2O)    IKE        EVAL-feb04 Keinert,Mattes                    '
' IKE 6-201 (2004)     DIST-feb04                       040202     '
'----IAEA-IKE          MATERIAL   11                                '
'-----THERMAL NEUTRON SCATTERING DATA                               '
'------ENDF-6 FORMAT                                               '
'*                                                                 *'
'*-------------------------------------------------------------------*'
'*  only incoherent scattering possible by LEAPR                    *'
'*       D-D interference scattering not included  <<<<<<<<<<<<<< *'
'*-------------------------------------------------------------------*'
'*  LEAPR/NJOY-99.90+          generated atIKE Stuttgart feb.2004 *'
/  end leapr input
stop
-------------------------------------------------------------------------
```

Nuclear Data Section
International Atomic Energy Agency
P.O. Box 100
A-1400 Vienna
Austria

e-mail: services@iaeand.iaea.org
fax: (43-1) 26007
cable: INATOM VIENNA
telex: 1-12645
telephone: (43-1) 2600-21710